[5] Bots ML, Hoes AW, Koudstaal PJ, Hofman A, Grobbee DE. Common carotid intima-media thickness and risk of stroke and myocardial infarction: the Rotterdam Study. Circulation 1997;96:1432–7.
[6] Touboul PJ, Elbaz A, Koller C, et al. Common carotid artery intima-media thickness and brain infarction: the Etude du Profil Genetique de l'Infarctus Cerebral (GENIC) case-control study. The GENIC Investigators. Circulation 2000;102:313–8.
[7] Yamasaki Y, Kawamori R, Matsushima H, et al. Atherosclerosis in carotid artery of young IDDM patients monitored by ultrasound high-resolution B-mode imaging. Diabetes 1994;43:634–9.
[8] Folsom AR, Eckfeldt JH, Weitzman S, et al. Relation of carotid artery wall thickness to diabetes mellitus, fasting glucose and insulin, body size, and physical activity. Atherosclerosis Risk in Communities (ARIC) Study Investigators. Stroke 1994;25:66–73.
[9] Kawamori R, Yamasaki Y, Matsushima H, et al. Prevalence of carotid atherosclerosis in diabetic patients. Ultrasound high-resolution B-mode imaging on carotid arteries. Diabetes Care 1992;15:1290–4.
[10] Minamikawa J, Tanaka S, Yamauchi M, Inoue D, Koshiyama H. Potent inhibitory effect of troglitazone on carotid arterial wall thickness in type 2 diabetes. J Clin Endocrinol Metab 1998;83:1818–20.
[11] Furberg CD, Adams Jr HP, Applegate WB, et al. Effect of lovastatin on early carotid atherosclerosis and cardiovascular events. Asymptomatic Carotid Artery Progression Study (ACAPS) Research Group. Circulation 1994;90:1679–87.
[12] Lonn E, Yusuf S, Dzavik V, et al. Effects of ramipril and Vitamin E on atherosclerosis: the study to evaluate carotid ultrasound changes in patients treated with ramipril and Vitamin E (SECURE). Circulation 2001;103:919–25.
[13] Kodama M, Yamasaki Y, Sakamoto K, et al. Antiplatelet drugs attenuate progression of carotid intima-media thickness in subjects with type 2 diabetes. Thromb Res 2000;97:239–45.
[14] Beishuizen ED, van de Ree MA, Jukema JW, et al. Two-year statin therapy does not alter the progression of intima-media thickness in patients with type 2 diabetes without manifest cardiovascular disease. Diabetes Care 2004;27:2887–92.
[15] Rantala AO, Paivansalo M, Kauma H, et al. Hyperinsulinemia and carotid atherosclerosis in hypertensive and control subjects. Diabetes Care 1998;21:1188–93.
[16] Kanai H, Hasegawa H, Ichiki M, Tezuka F, Koiwa Y. Elasticity imaging of atheroma with transcutaneous ultrasound: preliminary study. Circulation 2003;107:3018–21.
[17] Hasegawa H, Kanai H, Hoshimiya N, Koiwa Y. Evaluating the regional elastic modules of a cylindrical shell with nonuniform wall thickness. J Med Ultrason 2004;31:81–90.
[18] Kanai H, Sato M, Koiwa Y, Chubachi N. Transcutaneous measurement and spectrum analysis of heart wall vibrations. IEEE Trans Ultrason Ferroelectr Freq Control 1996;43:791–810.
[19] Kanai H, Koiwa Y, Zhang J. Real-time measurement of local myocardium motion and arterial wall thickening. IEEE Trans Ultrason Ferroelectr Freq Control 1999;46:1229–41.
[20] Hasegawa H, Kanai H, Hoshimiya N, Chubachi N, Koiwa Y. Accuracy evaluation in the measurement of a small change in the thickness of arterial walls and the measurement of elasticity of the human carotid artery. Jpn J Appl Phys 1998;37:3101–5.
[21] Kanai H, Hasegawa H, Chubachi N, Koiwa Y, Tanaka M. Noninvasive evaluation of local myocardinal thickening and its color-coded imaging. IEEE Trans Ultrason Ferroelectr Freq Control 1997;44:752–68.
[22] Salonen R, Seppanen K, Rauramaa R, Salonen JT. Prevalence of carotid atherosclerosis and serum cholesterol levels in eastern Finland. Arteriosclerosis 1988;8:788–92.
[23] Poli A, Tremoli E, Colombo A, et al. Ultrasonographic measurement of the common carotid artery wall thickness in hypercholesterolemic patients. A new model for the quantitation and follow-up of preclinical atherosclerosis in living human subjects. Atherosclerosis 1988;70:253–61.
[24] O'Leary DH, Polak JF, Kronmal RA, et al. Distribution and correlates of sonographically detected carotid artery disease in the Cardiovascular Health Study. The CHS Collaborative Research Group. Stroke 1992;23:1752–60.
[25] Handa N, Matsumoto M, Maeda H, et al. Ultrasonic evaluation of early carotid atherosclerosis. Stroke 1990;21:1567–72.
[26] Lehmann ED, Hopkins KD, Gosling RG. Increased aortic stiffness in women with NIDDM. Diabetologia 1996;39:870–1.
[27] Farrar DJ, Green HD, Wagner WD, Bond MG. Reduction in pulse wave velocity and improvement of aortic distensibility accompanying regression of atherosclerosis in the rhesus monkey. Circ Res 1980;47:425–32.
[28] Lehmann ED, Riley WA, Clarkson P, Gosling RG. Non-invasive assessment of cardiovascular disease in diabetes mellitus. Lancet 1997;350(Suppl. 1):SI14–9.
[29] Lantelme P, Mestre C, Lievre M, Gressard A, Milon H. Heart rate: an important confounder of pulse wave velocity assessment. Hypertension 2002;39:1083–7.

Am J Physiol Endocrinol Metab 294: E668–E678, 2008.
First published January 29, 2008; doi:10.1152/ajpendo.00640.2007.

Ambient glucose levels qualify the potency of insulin myogenic actions by regulating SIRT1 and FoxO3a in C_2C_{12} myocytes

Taku Nedachi,[1] Akito Kadotani,[1,3] Miyako Ariga,[1,2] Hideki Katagiri,[2,3] and Makoto Kanzaki[1,4]

[1]*Division of Biomaterials, Tohoku University Biomedical Engineering Research Organization;* [2]*21st COE program "CRESCENDO", Graduate School of Pharmaceutical Sciences;* [3]*Division of Advanced Therapeutics for Metabolic Diseases, Center for Translational and Advanced Animal Research; and* [4]*Center for Research Strategy and Support, Tohoku University, Sendai, Japan*

Submitted 3 October 2007; accepted in final form 18 January 2008

Nedachi T, Kadotani A, Ariga M, Katagiri H, Kanzaki M. Ambient glucose levels qualify the potency of insulin myogenic actions by regulating SIRT1 and FoxO3a in C_2C_{12} myocytes. *Am J Physiol Endocrinol Metab* 294: E668–E678, 2008. First published January 29, 2008; doi:10.1152/ajpendo.00640.2007.—Nutrition availability is one of the major environmental signals influencing cell fate, such as proliferation, differentiation, and apoptosis, often functioning in concert with other humoral factors, including insulin. Herein, we show that low-serum-induced differentiation of C_2C_{12} myocytes is significantly hampered under low glucose (LG; 5 mM) compared with high glucose (HG; 22.5 mM) conditions, concurrently with nuclear accumulation of SIRT1, an NAD^+-dependent deacetylase, and FoxO3a, both of which are implicated in the negative regulation of myogenesis. Intriguingly, insulin appears to exert opposite actions, depending on glucose availability, with regard to the regulation of SIRT1 and FoxO3a abundance, which apparently contributes to modulating the potency of insulin's myogenic action. Namely, insulin exerts a potent myogenic effect in the presence of sufficient glucose, whereas insulin is unable to exert its myogenic action under LG conditions, since insulin evokes massive upregulation of both SIRT1 and FoxO3a in the absence of sufficient ambient glucose. In addition, the hampered differentiation state under LG is significantly restored by sirtinol, a SIRT1 inhibitor, whereas insulin abolished this sirtinol-dependent restoration, indicating that insulin can function as a negative as well as a positive myogenic factor depending on glucose availability. Taken together, our data reveal the importance of ambient glucose levels in the regulation of myogenesis and also in the determination of insulin's myogenic potency, which is achieved, at least in part, through regulation of the cellular contents and localization of SIRT1 and FoxO3a in differentiating C_2C_{12} myocytes.

forkhead box O; differentiation

SKELETAL MUSCLE CELLS have provided a useful model for exploring the molecular mechanisms involved in cellular differentiation (13), and insulin and insulin-like growth factors (IGFs) have been implicated in the process of myogenesis by activating the IRS-PI 3-kinase signaling pathway (7, 22, 25, 53) that also serves as a pivotal intracellular signal for exerting metabolic actions in mature skeletal muscle (9). However, despite our general understanding of the effects of ambient glucose levels on insulin responsiveness with regard to metabolic actions in skeletal muscle cells (37), the possible interrelationship between glucose and insulin acting on myogenesis remains to be clarified.

Skeletal muscle differentiation is a well-organized process governed by muscle-specific transcription factors belonging to the MyoD family, such as MyoD and myogenin (42), and the myocyte enhancer factor-2 (MEF2) family, such as MEF2A and MEF2C (35). In addition to these muscle-specific transcription factors, positively regulating myogenesis, the forkhead box O (FoxO) class of transcription factors, ubiquitously expressed in various cell types, has been shown to negatively regulate myogenesis (27). Insulin/IGF-induced repression of FoxO transcription factors, resulting from their nuclear exclusion in response to Akt-mediated phosphorylation, has been implicated in a key aspect of insulin/IGF actions not only for stimulating myogenesis but also for preventing muscle atrophy (21, 46).

Myogenesis is also directly influenced by the acetylation status of histones and nonhistone proteins including MyoD and MEF2, and class I and II histone deacetylases (HDACs) have been shown to regulate muscle gene expression by inhibiting MyoD and MEF2 factors (31, 33, 43). Recently, silent information regulator-2 (Sir2), a class III deacetylase originally characterized as controlling the life spans of animals in response to nutritional availability, was also identified to serve as a key regulator for myogenesis (14) via overexpression of SIRT1, the mammalian ortholog for Sir2, in C_2C_{12} myoblasts by strongly inhibiting differentiation into myotubes, whereas suppression of SIRT1 expression by RNA interference enhanced myogenesis (14).

Given the unique property of SIRT1 that the cofactor nicotinamide adenine dinucleotide (NAD^+) drives deacetylation activity, SIRT1 has been thought to serve as an energy and/or oxidation sensor, being directly involved in the nutritional regulation of gene transcription events in various tissues including skeletal muscle (38, 40, 45). Intriguingly, recent studies have also demonstrated that SIRT1 controls cellular functions by deacetylating FoxO transcription factors in response to various stimuli including nutritional availability (4, 36, 38). Thus, myogenesis is likely to be regulated cooperatively by SIRT1 serving as a sensor of the nutritional environment in concert with FoxOs serving as an insulin/IGF sensor in various situations in which glucose and insulin levels are fluctuating. However, no data are available on the potential interplay between ambient glucose levels and insulin in the regulations of SIRT1 and FoxOs, or on the regulation of myogenesis.

Address for reprint requests and other correspondence: M. Kanzaki, Center for Research Strategy and Support (CRESS), Tohoku University, 2-1 Seiryo-machi, Aoba-ku, Sendai 980-8575, Japan (e-mail: Kanzaki@tubero.tohoku.ac.jp).

The costs of publication of this article were defrayed in part by the payment of page charges. The article must therefore be hereby marked "*advertisement*" in accordance with 18 U.S.C. Section 1734 solely to indicate this fact.

To gain insight into these issues, we investigated the effects of ambient glucose levels on differentiation of C_2C_{12} myocytes and found the potency of insulin's myogenic action to be remarkably affected by extracellular glucose levels and that insulin exerts its maximum myogenic effect only in the presence of a relatively high level of glucose, whereas its potency is significantly compromised under low glucose (LG) conditions, a state in which massive upregulations of SIRT1 and FoxO3a are induced by insulin treatment. Thus, these findings reveal an important interplay between ambient glucose and insulin favoring alterations in the cellular contents of SIRT1 and FoxO3a, both of which are tightly coupled to the regulation of myogenesis.

MATERIALS AND METHODS

Materials. The Western blot detection kit (West super femto detection reagents) was obtained from Pierce Biotechnology (Rockford, IL). Dulbecco's modified Eagle's medium (DMEM), penicillin-streptomycin and trypsin-EDTA were purchased from Sigma Chemicals (St. Louis, MO). Cell culture equipment was from BD Biosciences (San Jose, CA). Calf serum (CS) and fetal bovine serum (FBS) were obtained from BioWest (Nuaille, France). Immobilon-P and anti-SIRT1 antibody were from Millipore (Bedford, MA). Anti-myosin heavy chain (MHC; MF20) and anti-myogenin (F5D) antibodies were obtained from Iowa Hybridoma Bank (University of Iowa, Iowa City, IA). Anti-phospho-S6 ($Ser^{235/236}$), anti-Akt, anti-phospho-Akt (Ser^{473}), and anti-phospho Akt (Thr^{308}) antibodies were purchased from Cell Signaling Technology (Danvers, MA). Anti-β-actin antibody was obtained from Sigma Chemicals. Unless otherwise noted, all chemicals were of the purest grade available from Sigma Chemicals.

Cell culture. Mouse skeletal muscle cell line C_2C_{12} myoblasts (54) were maintained in DMEM supplemented with 10% FBS, 30 μg/ml penicillin, and 100 μg/ml streptomycin (growth medium) at 37°C under a 5% CO_2 atmosphere. For biochemical study, the cells were grown on 4-well plates (Nalgen Nunc International, Rochester, NY) at a density of 1×10^5 cells/well in 5 ml of growth medium or on 6-well plates (BD Biosciences) at a density of 3×10^4 cells/well in 3 ml of growth medium. Three days after plating, cells had reached ~80–90% confluence (*day 0*). Differentiation was then induced by switching the growth medium to DMEM supplemented with 2% CS, 30 μg/ml penicillin, and 100 μg/ml streptomycin (differentiation medium). The differentiation medium was changed every 24 h. For the immunofluorescent staining study, cells were grown on 22-mm glass coverslips (C022221; Matsunami, Osaka, Japan) in 6-well plates.

Immunofluorescent studies. C_2C_{12} myoblasts were cultured on coverslips placed on 6-well plates. After differentiation, the cells were stimulated with 100 nM insulin for 60 min. Then, the cells were fixed with 2% paraformaldehyde in PBS (without Ca^{2+} and Mg^{2+}), followed by immunocytochemistry using anti-SIRT1 antibody (Millipore), and anti-mouse IgG antibody conjugated with Alexa 555 or Alexa 594 (Invitrogen, Carlsbad, CA). Images were monitored and analyzed using Olympus Fluoview FV1000 confocal microscopy and the associated application program, ASW v. 1.3 (Olympus, Tokyo, Japan).

Nuclear extract preparation. Nuclear extract preparation was performed as follows. Briefly, the cells were washed three times with PBS (-) and resuspended in *buffer A* (10 mM HEPES-OH, pH 7.9, 1.5 mM $MgCl_2$, 10 mM KCl). After a 20-min incubation on ice, the cells were destroyed with a vortex mixer (maximum speed), and the pellets were then collected. The pellets were resuspended in 50 μl of *buffer C* (HEPES-OH, pH 7.9, 420 mM NaCl, 1.5 mM $MgCl_2$, 0.2 mM EDTA, 25% glycerol) and then frozen (−80°C) and thawed twice. The supernatants were collected as nuclear extracts, and the protein concentration was measured and then stored at −80°C until Western blot analysis.

Immunoprecipitation. The cell lysates were prepared using Triton X-100-NP40 lysis buffer (50 mM Tris-Cl, 150 mM NaCl, 1 mM EDTA, 1% Triton X-100, 1% NP-40) and the protein concentrations of each sample were measured using a bicinchoninic acid assay (BCA) protein assay kit (Pierce). Five hundred micrograms of protein were mixed with 2 μg of anti-SIRT1 polyclonal antibody. The mixtures were incubated at 4°C for 3 h and continuously incubated in the presence of protein A-Sepharose. The immunoprecipitates were washed with Triton X-100-NP-40 lysis buffer three times. The adsorbed proteins were eluted with 1× Laemmli's buffer, boiled, and subjected to Western blot analysis.

Western blot analysis. The expression and phosphorylation of each protein were analyzed by Western blot analysis. In brief, the harvested cell lysates were subjected to 5% or 12% SDS-polyacrylamide gel electrophoresis (1:30 bis:acrylamide). Proteins were transferred to a PVDF membrane (Immobilon-P, Millipore), and the membranes were then blocked for 2 h at room temperature with 5% nonfat dry milk in Tris-buffered saline (TBS) containing 0.1% Tween-20. Immunostaining to detect each protein was achieved with a 1-h incubation with a 1:1,000 dilution of anti-SIRT1 antibody, anti-myosin heavy chain antibody, and anti-myogenin antibody. Specific totals or phosphoproteins were visualized after subsequent incubation with a 1:5,000 dilution of anti-mouse or rabbit IgG conjugated to horseradish peroxidase and a SuperSignal chemiluminescence detection procedure (Pierce Biotechnology). Protein concentrations were determined using a BCA assay. Three independent experiments were performed for each condition. Coomassie blue staining was also performed to assess the efficiency of protein transfer.

Real-time PCR. Fluorescence real-time PCR analysis was performed using a Light Cycler instrument and SYBR Green detection kit according to the manufacturer's instructions (Roche Diagnostics, Indianapolis, IN). PCR primers for measuring each of the secreted factors were as follows: for SIRT1, 5′-GAT CCT TCA GTG TCA TGG TT-3′ and 5′-GAA GAC AAT CTC TGG CTT CA-3′; for FoxO3a, 5′-TGC CTT GTC AAA TTC TGT C-3′ and 5′-TGC ACT AGC TGA ATA CAG TGA G-3′; for GAPDH, 5′-GGA GAA ACC TGC CAA GTA TGA-3′ and 5′-GCA TCG AAG GTG GAA GAG T-3′.

Glucose concentration assay. Glucose concentrations in the cultured media were measured using a determiner GLE kit (Kyowa Medex, Tokyo, Japan).

Statistical analysis. Statistical analysis was performed using one-way ANOVA followed by Tukey's multiple comparison test or Student's paired *t*-test for independent samples. Data are expressed as means ± SE unless otherwise specified.

RESULTS

Extracellular glucose influences low-serum-induced C_2C_{12} differentiation. To characterize the effects of extracellular glucose levels on myogenesis of C_2C_{12} cells, we first examined whether the glucose concentration in the low-serum differentiation medium (DMEM + 2% CS) affects C_2C_{12} differentiation. Under the LG (5 mM glucose) conditions, the process of myogenesis was obviously delayed and the number of well-developed myotubes was decreased compared with high glucose (22.5 mM glucose; HG) conditions on *day 4* of differentiation (Fig. 1*A*). We quantified differentiation status by counting the number of myotubes defined as multinuclear myotubes that contained more than 5 nuclei (Fig. 1*B*), as we previously reported (37). The effect of the extracellular glucose concentration on myogenesis was confirmed by Western blot analysis of differentiation marker proteins using anti-skeletal muscle type MHC and anti-myogenin antibodies, as not only were their expressions detected later, but their amounts were also

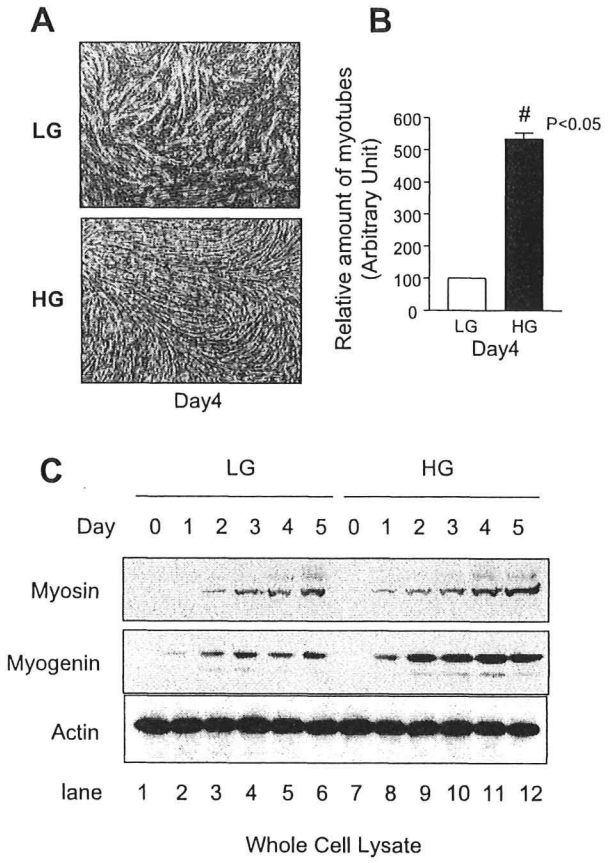

Fig. 1. Low-serum-induced C_2C_{12} myoblast differentiation was affected by extracellular glucose levels. *A* and *B*: C_2C_{12} myoblasts were cultured in low glucose (LG)-DMEM (5 mM glucose) + 10% FBS and then switched to differentiation medium [DMEM + 2% calf serum (CS); D-medium] containing 5 mM (LG) or 22.5 mM high glucose (HG) glucose (*day 0*). Cells were continuously cultured with D-medium changes every 24 h. *A*: at *day 4* of differentiation under LG (*a*) or HG (*b*) conditions, myotube formations were observed under a microscope. *B*: relative numbers of myotubes, defined as multinuclear myotubes containing more than 5 nuclei, were determined. Statistical analysis was performed using paired *t*-test. #$P < 0.05$ ($n = 5$). *C*: on the indicated day, cell lysates were prepared, and the same amounts of proteins were subjected to Western blotting using anti-myosin, anti-myogenin, and anti-β-actin antibodies. Each experiment was repeated 3 times and representative results are shown.

lower than in C_2C_{12} cells differentiated under LG conditions (Fig. 1*C*).

SIRT1 predominantly localizes in the nucleus under LG conditions but is excluded under HG conditions in C_2C_{12} myotubes. To understand the mechanisms by which extracellular glucose alters the process of C_2C_{12} differentiation, we initially focused on SIRT1, an NAD-dependent protein deacetylase with enzymatic activity sensitive to changes in cellular energy levels (for a review, see Ref. 2), since a recent study showed direct involvement of SIRT1 in myogenesis (14). Consistent with previous reports showing that Sir2 and its mammalian homolog SIRT1 are localized in the nucleus (19, 34), immunofluorescent analysis using anti-SIRT1 antibody demonstrated that, when C_2C_{12} cells were differentiated under LG conditions, predominant localization of SIRT1 was observed in the nucleus (Fig. 2*A*, *a*) similar to what was observed in undifferentiated myoblasts (data not shown). In contrast, when C_2C_{12} myoblasts were differentiated under HG conditions, the number of SIRT1-positive nuclei was remarkably reduced (Fig. 2*A*, *c*, see arrowheads), as confirmed by Western blotting analysis of nuclear proteins extracted under each culture condition (data not shown). Counterstaining was performed with DAPI (Fig. 2*A*, *b* and *d*). Immunofluorescent analysis demonstrated that the nuclear exclusion of SIRT1 was not acutely induced by HG administration in either myoblasts (data not shown) or LG-differentiated myotubes (Fig. 2*B*). However, we found that total SIRT1 protein was significantly reduced when C_2C_{12} cells were differentiated under HG conditions (Fig. 2*C*, *bottom*, HG-SIRT1) compared with those under LG conditions (*top*, LG-SIRT1). The HG-dependent reduction of SIRT1 was obvious from *day 2* of differentiation (Fig. 2*C*, *bottom*, HG-SIRT1, *lane3*).

Myogenesis is a highly organized and regulated sequence of multiple processes orchestrated by a wide variety of functional proteins, including SIRT1, requiring a relatively long time, and all of these processes could be affected by ambient glucose levels. In an attempt to dissect the effects of glucose on SIRT1 regulation and myogenesis, we conducted an experiment to specify the time required for glucose to exert its effect on SIRT1 suppression. Thus, C_2C_{12} myotubes differentiated under LG conditions (*days 5–6*) were transferred to HG or the same LG medium, and time course changes in SIRT1 contents were analyzed by Western blotting (Fig. 2, *D* and *E*). The time course experiment revealed that 24-h exposure to HG is sufficient for reducing the cellular SIRT1 content and its nuclear localization (data not shown) in LG-differentiated C_2C_{12} myotubes. In addition, we performed the converse experiments; that is, C_2C_{12} myotubes were cultured under HG conditions and then switched to LG for the indicated time to confirm that amounts of SIRT1 were reversibly controlled by ambient glucose levels (Fig. 2*F*). We also measured SIRT1 mRNA levels under these conditions and found that SIRT1 mRNA was significantly induced by switching to the LG condition ($P < 0.05$, $n = 4$; Fig. 2*G*). Thus, these results suggest that SIRT1 protein induction is regulated, at least in part, by its mRNA levels.

FoxO3a localizes in predominantly the nucleus under LG conditions but is excluded under HG conditions in C_2C_{12} myotubes. We next examined whether FoxO3a associates with the spatiotemporal changes in SIRT1 localization in response to alterations in glucose availability, since recent reports revealed functional and physical interactions between SIRT1 and FoxO transcription factors in response to various stimuli including oxidative stress (4, 36) and nutritional circumstances (38). Similar to the pattern observed in SIRT1 subcellular localization, FoxO3a was predominantly detected in the nuclei of myotubes when the cells were differentiated under LG conditions (Fig. 3*A*, *a*), whereas no nuclear localization of FoxO3 was observed in those differentiated under HG conditions (Fig. 3*A*, *c*). Again, HG administration failed to induce acute redistribution of FoxO3a (Fig. 3*B*) but resulted in a remarkable reduction of FoxO3a when the LG-differentiated myotubes (*days 5* and *6*) were exposed to HG for an additional 24 h (Fig. 3, *D* and *E*). Furthermore, we confirmed that FoxO3a protein was reversibly controlled by extracellular glucose (Fig. 3*F*) and also that FoxO3a mRNA levels were regulated by

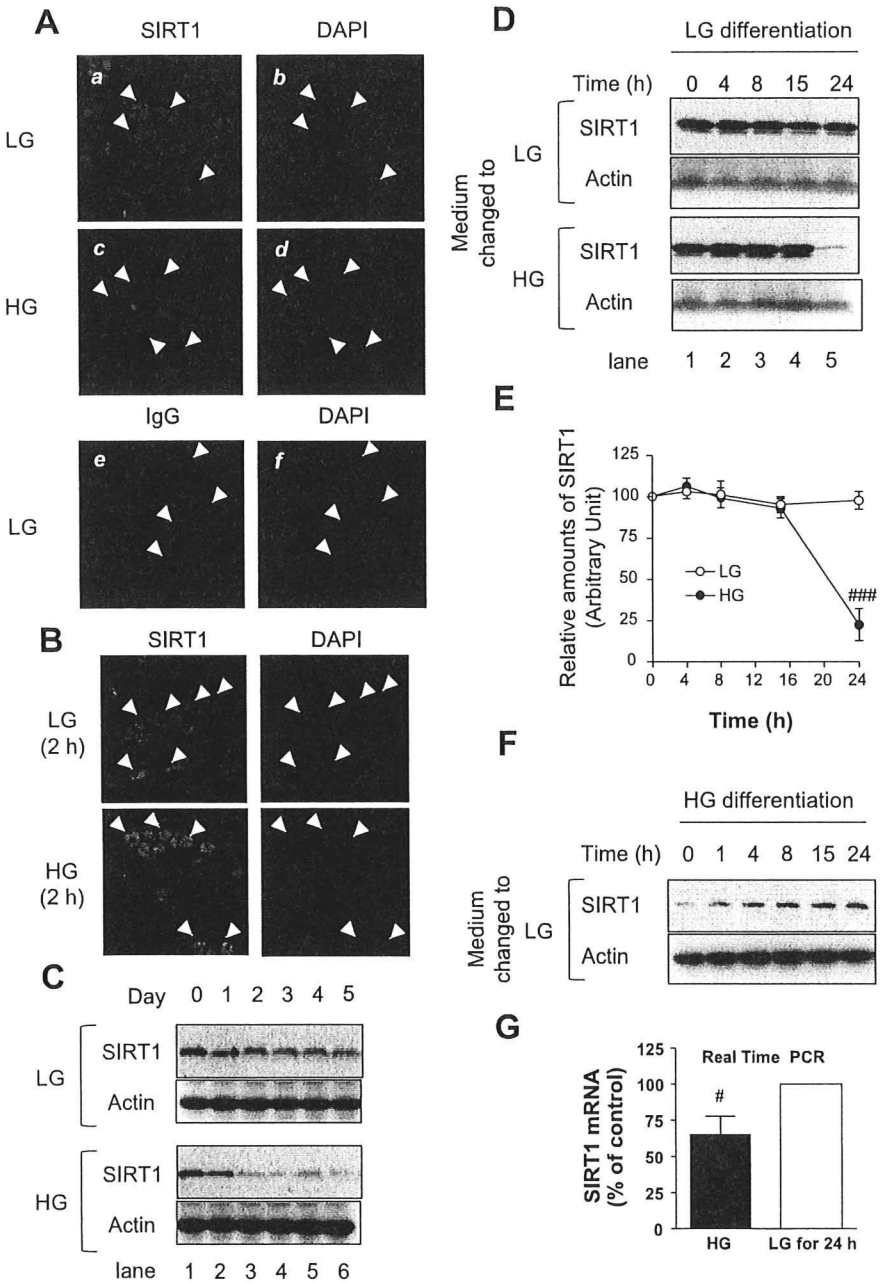

Fig. 2. Cellular abundance of SIRT1 and its localization are controlled by extracellular glucose levels during myogenesis. *A*: C_2C_{12} myoblasts were differentiated into myotubes under LG conditions (5 mM glucose in DMEM + 2% CS) or HG conditions (22.5 mM glucose in DMEM + 2% CS) for 6 days. Myotubes were then fixed and immunostained using anti-SIRT1 antibody (*a, c*) or anti-IgG as a negative control (*e*). DAPI staining was performed at the same time to confirm the position of the nucleus (*b, d, f*). *B*: C_2C_{12} myoblasts were differentiated into myotubes under LG conditions for 6 days. Myotubes were then incubated under LG or HG conditions for 2 h. Cells were fixed and immunostained using anti-SIRT1 antibody and DAPI. *C*: C_2C_{12} myoblasts were differentiated into myotubes under LG or HG conditions for the indicated days. Cell lysates were prepared as described in MATERIALS AND METHODS, and the same protein samples were subjected to Western blotting using anti-SIRT1 antibody. *D*: C_2C_{12} myoblasts were differentiated into myotubes under LG conditions for 6 days. Next, media were switched to LG or HG conditions, and myotubes were then further incubated for the indicated times. Cell lysates were prepared as described in MATERIALS AND METHODS, and the same protein amounts were subjected to Western blotting using anti-SIRT1 antibody. *E*: densitometric analysis of *D*. Statistical analysis was performed using 1-way ANOVA, as described in MATERIALS AND METHODS [$\#\#\#P < 0.001$ vs. control (0 h), HG, $n = 3$]. *F* and *G*: C_2C_{12} myoblasts were differentiated into myotubes under HG conditions for 6 days. Next, media were switched to LG conditions, and myotubes were then further incubated for the indicated time. *F*: cell lysates were subjected to Western blotting using anti-SIRT1 antibody. *G*: total RNAs were purified and subjected to real-time PCR analysis to measure SIRT1 mRNA amounts as described in MATERIALS AND METHODS. Statistical analysis was performed using paired *t*-test ($\#P < 0.05$, $n = 3$). All experiments were performed at least 3 times, and similar results were obtained.

extracellular glucose ($P < 0.001$, $n = 4$; Fig. 3*G*). Thus, FoxO3a displayed spatiotemporal regulation similar to that observed in SIRT1 in response to altered extracellular glucose levels. However, the changes in cellular FoxO3a content during myogenesis were obviously different from those of SIRT1. As shown in Fig. 3*C*, little FoxO3a expression was observed in undifferentiated myoblasts (*day 0*), but its expression gradually increased upon differentiation only under LG conditions. This differentiation-dependent increase in the cellular content of FoxO3a was abolished when the cells were differentiated under HG conditions.

Taken together, these data demonstrate that, although acute HG treatment fails to induce subcellular redistributions of SIRT1 and FoxO3a, with chronic HG treatment (24 h) there is an obvious nuclear exclusion of these proteins concomitant with the significant reductions in their cellular contents in differentiating C_2C_{12} cells. These data also suggest the compromised myogenesis under LG conditions to be attributable to nuclear accumulation of relatively high levels of SIRT1 and FoxO3a in C_2C_{12} cells. In addition, our data indicate that 24-h exposure to HG is sufficient to produce obvious reductions in both SIRT1 and FoxO3a proteins in C_2C_{12} myotubes.

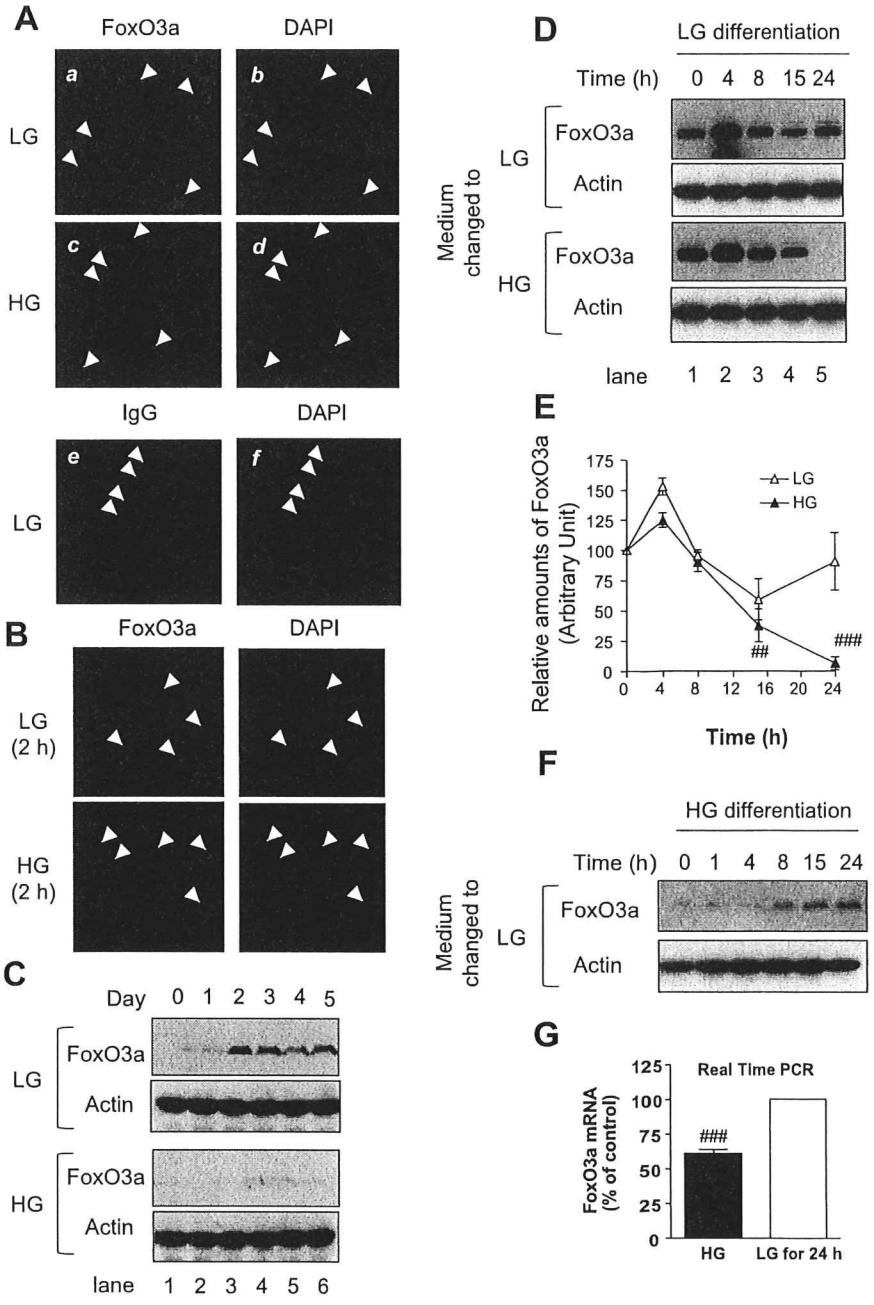

Fig. 3. Cellular abundance of FoxO3a and its localization are controlled by extracellular glucose levels during myogenesis. *A*: C_2C_{12} myoblasts were differentiated into myotubes under LG conditions (5 mM glucose in DMEM + 2% CS) or HG conditions (22.5 mM glucose in DMEM + 2% CS) for 6 days. Myotubes were then fixed and immunostained using anti-FoxO3a antibody (*a, c*) or anti-IgG as a negative control (*e*). DAPI staining was performed at the same time to confirm the position of the nucleus (*b, d, f*). *B*: C_2C_{12} myoblasts were differentiated into myotubes under LG conditions for 6 days. Myotubes were then incubated under LG or HG conditions for 2 h. Cells were fixed and immunostained using anti-FoxO3a antibody and DAPI. *C*: C_2C_{12} myoblasts were differentiated into myotubes under LG or HG conditions for the indicated days. Cell lysates were prepared as described in MATERIALS AND METHODS, and the same protein amounts were subjected to Western blotting analysis using anti-FoxO3a antibody. *D*: C_2C_{12} myoblasts were differentiated into myotubes under LG conditions for 6 days. Next, media were switched to LG or HG conditions, and myotubes were then further incubated for the indicated time. Cell lysates were subjected to Western blotting analysis using anti-FoxO3a antibody. *E*: densitometric analysis of *D*. Statistical analysis was performed using 1-way ANOVA followed by Tukey's posttest [$\#\#P < 0.01$, $\#\#\#P < 0.001$, $n = 3$) vs. control (0 h, HG)]. *F* and *G*: C_2C_{12} myoblasts were differentiated into myotubes under HG conditions for 6 days. Next, media were switched to LG conditions, and myotubes were then further incubated for the indicated time. *F*: cell lysates were subjected to Western blotting using anti-FoxO3a antibody. *G*: total RNA was purified and subjected to real-time PCR analysis to measure FoxO3a mRNA amounts as described in MATERIALS AND METHODS. Statistical analysis was performed using paired *t*-test ($\#\#\#P < 0.001$, $n = 3$). All experiments were performed at least 3 times, and similar results were obtained.

Extracellular glucose levels modify the stimulatory effect of insulin on myogenesis by altering cellular contents of SIRT1 and FoxO3a. Effects of HG appeared to be elicited within 24 h as assessed by the obvious reductions of both SIRT1 and FoxO3a proteins in the LG-differentiated C_2C_{12} myotubes (Figs. 2 and 3). We therefore took advantage of this phenomenon to explore the possible interplay between insulin and ambient glucose during the regulation of myogenesis. Namely, the LG-differentiated C_2C_{12} myotubes (*days 5* and *6*) were transferred to LG or HG medium in the absence or presence of the indicated insulin concentration and cultured for an additional 24 h, and the cellular contents of SIRT1 and FoxO3a were then analyzed by Western blotting (Fig. 4). In the presence of LG, insulin significantly increased cellular contents of both SIRT1 (Fig. 4*A*, *top, lanes 1–6*) and FoxO3a (Fig. 4*A*, *middle, lanes 1–6*) in a dose-dependent manner (Fig. 4, *B* and *C*, open symbols) although the amount of β-actin as a loading control was not changed (Fig. 4*A*, *bottom*). In the presence of insulin under LG conditions for 24 h, SIRT1 predominantly displayed nuclear localization, whereas increased FoxO3a displayed both cytoplasmic and nuclear localization (data not shown). In sharp contrast, insulin treatment tended to decrease

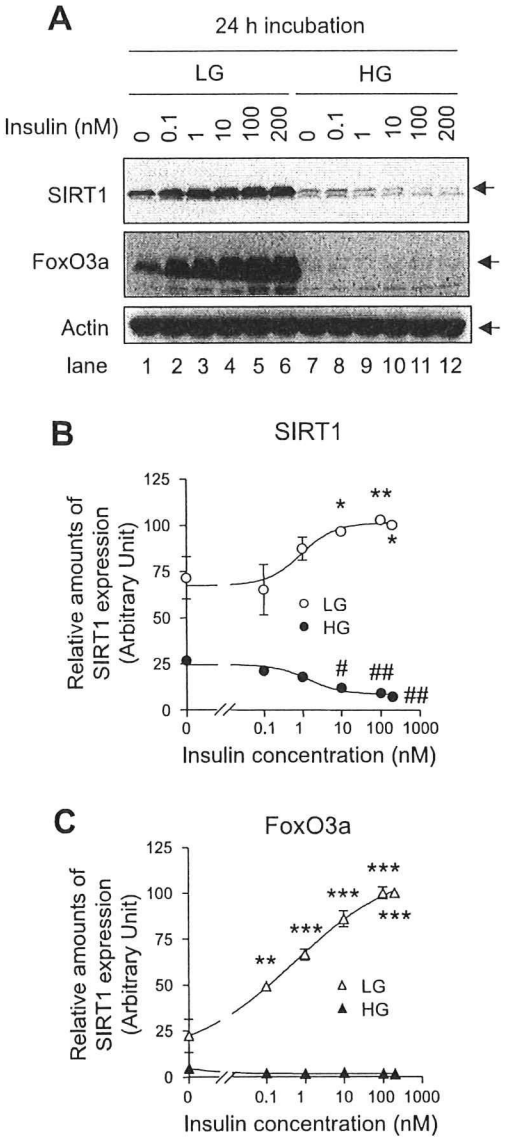

Fig. 4. Effects of insulin on SIRT1 and FoxO3a abundances depend on extracellular glucose levels. *A*: C_2C_{12} myoblasts were differentiated into myotubes under LG conditions for 6 days. Then, media were switched to HG (22.5 mM glucose in DMEM + 2% CS) or control LG (5 mM glucose in DMEM + 2% CS) in the presence or absence of the indicated concentration of insulin for 24 h. Amounts of SIRT1, FoxO3a, and β-actin were monitored by Western blotting. *B*: densitometric analysis of SIRT1 abundance during time course experiments. Statistical analysis was performed using 1-way ANOVA followed by Tukey's posttest [$*P < 0.05$, $**P < 0.01$ ($n = 3$) vs. LG control (LG, 0 nM insulin); $\#P < 0.05$, $\#\#P < 0.01$ ($n = 3$) vs. HG control (HG, 0 nM insulin)]. *C*: densitometric analysis of FoxO3a abundance during time course experiments. Statistical analysis was performed using 1-way ANOVA followed by Tukey's posttest [LG: $*P < 0.05$, $**P < 0.01$, $***P < 0.001$ ($n = 3$) vs. LG control (LG, 0 nM insulin)].

SIRT1 protein in the presence of HG (Fig. 4*A*, *top, lanes 7–12*, and Fig. 4*B*, ●). Moreover, insulin completely failed to increase FoxO3a contents in the presence of HG (Fig. 4*A*, *bottom, lanes 7–12*; Fig. 4*C*, ▲). In the presence of insulin under HG conditions for 24 h, both of these proteins were barely detectable by immunofluorescent staining (data not shown).

To address the possibility that these changes in SIRT1 and FoxO3a proteins induced by the combined actions of insulin and glucose contribute to regulating the differentiation status of C_2C_{12} myotubes, the amount of MHC as a myogenic differentiation marker under each condition was also analyzed by Western blotting (Fig. 5). Consistent with the results depicted in Fig. 1, the stimulatory effect of HG on MHC expression was also detected even after incubation for just 24 h with HG (Fig. 5*A*, *lane 1* vs. *lane 6*). In the presence of HG, insulin displayed a potent myogenic-stimulating action, and MHC amounts were significantly increased in response to 100 nM insulin ($P < 0.05$, $n = 3$; Fig. 5*A*, *lanes 6–10*) under conditions in which the SIRT1 and FoxO3a contents were marginal (Fig. 4). In contrast, the myogenic stimulating potency of insulin was apparently limited (Fig. 5*A*, *lanes 1–5*) under LG conditions in which massive amounts of SIRT1 and FoxO3a were expressed (Fig. 4). The synergistic action of insulin and HG on the upregulation of MHC was clearly demonstrated by a quantitative densitometric analysis (Fig. 5*B*).

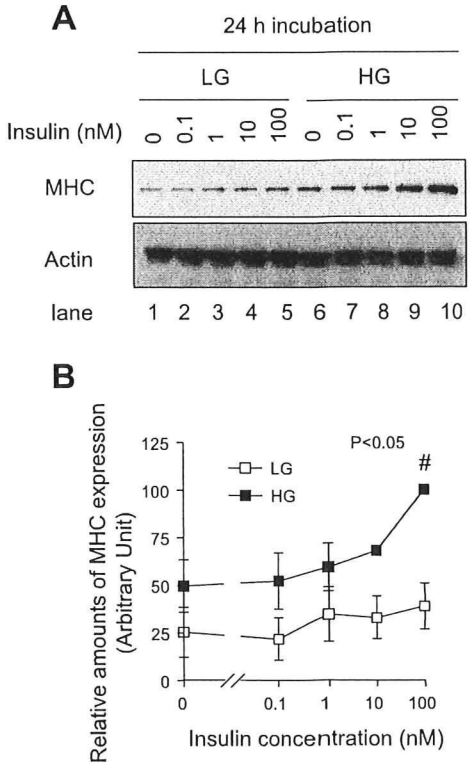

Fig. 5. Insulin myogenic potency is altered by extracellular glucose levels. *A*: C_2C_{12} myoblasts were differentiated into myotubes under LG conditions for 6 days. Then, media were switched to HG (22.5 mM glucose in DMEM + 2% CS) or control LG (5 mM glucose in DMEM + 2% CS) in the presence or absence of indicated concentration of insulin for 24 h. Amounts of myosin heavy chain (MHC) were monitored by Western blotting. *B*: densitometric analysis of *A*. Statistical analysis was performed using 1-way ANOVA followed by Tukey's posttest [HG: $\#P < 0.05$ ($n = 3$) vs. control (HG, 0 nM insulin)].

Glucose-dependent opposing effects of insulin on SIRT1 and FoxO3a are achieved through PI 3-kinase and mTOR activities. The myogenic action of insulin/IGFs has been shown to be mediated through the activation of PI 3-kinase and Akt signaling pathways (7, 23, 25, 53). In addition, several lines of evidence have demonstrated mTOR involvement in myogenesis (39, 47). To test whether the activities of PI 3-kinase and mTOR are involved in the regulation of SIRT1 and FoxO3a contents in response to insulin under LG or HG conditions, we used LY-294002 and rapamycin, potent inhibitors of PI 3-kinase and mTOR, respectively. Consistent with previous reports (8, 26, 41), the myogenic action of insulin as assessed by MHC expression, clearly detectable only in the presence of HG, was completely abolished by these compounds (Fig. 6, *A* and *C*, *bottom, lanes 4–6*). Importantly, these compounds also inhibited the insulin-mediated suppression of SIRT1 while increasing its cellular content during 24-h HG exposure (Fig. 6, *A* and *C*, *top, lanes 4–6*). Interestingly, these compounds were also effective under LG conditions and completely abolished insulin's action (Fig. 6, *A* and *C*, *middle,*

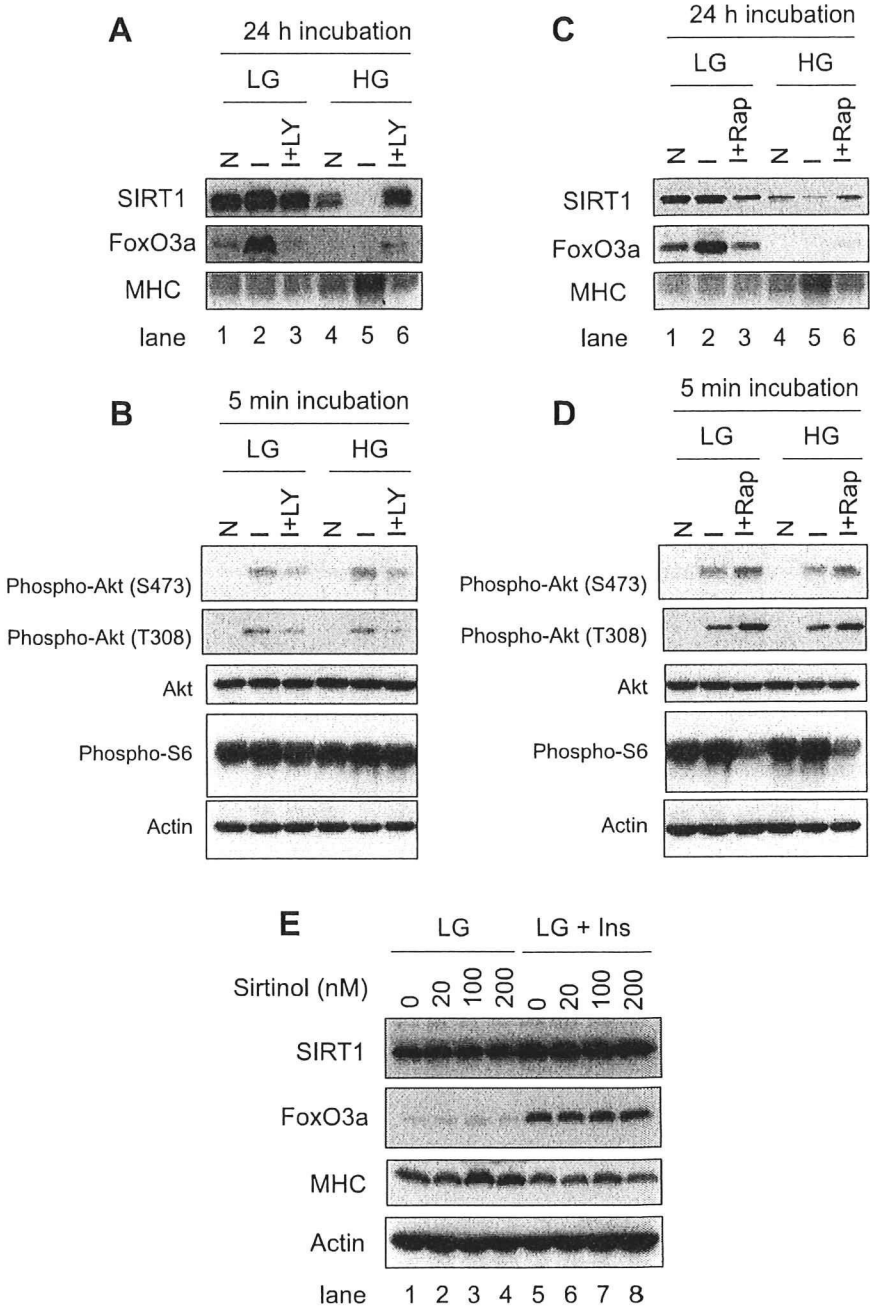

Fig. 6. Dissecting the interplay between glucose and insulin effects on SIRT1 and FoxO3a expressions and their involvements in myogenesis. *A* and *C*: C_2C_{12} myoblasts were differentiated into myotubes under LG conditions for 6 days. Media were then switched to HG or LG with or without 100 nM insulin in the presence or absence of 10 μM LY-294002 (*A*) or 50 nM rapamycin (*C*) for 24 h. Amounts of MHC, SIRT1, and FoxO3a were monitored by Western blotting. *B* and *D*: C_2C_{12} myoblasts were differentiated into myotubes under LG conditions for 6 days. Then, myotubes were treated with 100 nM insulin for 5 min in the presence or absence of 10 μM LY-294002 (*B*) or 50 nM rapamycin (*D*) under LG or HG conditions. Phosphorylations of Akt (Ser^{473} and Thr^{308}) and S6 as well as total Akt and β-actin were analyzed by Western blotting. *E*: C_2C_{12} myoblasts were differentiated into myotubes under LG conditions for 6 days. Cells were then cultured for 24 h in the presence of indicated concentrations of sirtinol under LG conditions (*lanes 1–4*) or LG + 100 nM insulin (*lanes 5–8*). Amounts of MHC, SIRT1, and FoxO3a were monitored by Western blotting. All experiments were repeated at least 3 times, and representative results are shown.

lanes 1–3), although insulin exerted completely opposing effects on the regulation of SIRT1 and FoxO3a abundances (Fig. 6, *A* and *B*, *top* and *middle*, *lane 2* vs. *lane 5*). We also monitored insulin-dependent phosphorylations of Akt and S6 in the presence of LY-294002 and rapamycin (Fig. 6, *B* and *D*). As expected, LY-294002 abolished insulin-dependent phosphorylation of Akt (Ser^{473} and Thr^{308}); on the other hand, rapamycin tended to increase insulin-dependent Akt phosphorylation (Fig. 6, *B* and *D*, *panels 1* and *2*) as previously reported (52). Phosphorylation of S6 was high under basal conditions but was slightly induced by insulin, and either LY-294002 or rapamycin had a negative effect on this phosphorylation (Fig. 6, *B and D*, *panel 4*).

Reduction of SIRT1 activity is not sufficient to restore C_2C_{12} differentiation status in the presence of insulin. Finally, we attempted to restore the poor differentiation seen under LG conditions by exposure to sirtinol, an inhibitor of SIRT1 (20, 32). Consistent with a previous study (14), 24-h exposure to sirtinol under LG conditions restored MHC expression to levels comparable to those observed in HG-exposed C_2C_{12} myotubes (Fig. 6*E*, *panel 3, lanes 1–4*). However, sirtinol failed to restore MHC expression (Fig. 6*E*, *panel 3, lanes 5–8*) in the presence of insulin, a condition in which FoxO3a is highly expressed (Fig. 6*E*, *panel 2, lanes 5–8*).

Changes in extracellular glucose levels during the course of overnight incubation. To precisely document the importance of ambient glucose levels in the phenomena described above, extracellular glucose concentrations were monitored during the course of overnight incubation of differentiated C_2C_{12} myotubes. As shown in Fig. 7, extracellular glucose levels gradually decreased but remained at high levels (~13 mM) even after an 18-h incubation when differentiated C_2C_{12} myotubes were cultured in HG-DMEM, whereas glucose in the medium was almost completely exhausted when the cells were cultured in LG-DMEM for 18 h.

DISCUSSION

In the present study, we demonstrated that low-serum-induced differentiation of C_2C_{12} cells is significantly influenced by extracellular glucose levels (Fig. 1), concurrently with glucose-dependent alterations in the amounts and subcellular localizations of SIRT1 and FoxO3a (Figs. 2 and 3) both of which have recently been implicated as negative regulators of myogenesis (14) (21). Consistent with many previous reports studying myogenesis by using mostly IGFs (6, 7, 12), insulin also exerts a myogenic action in a manner dependent on PI 3-kinase and mTOR activities, as assessed by MHC expression (Fig. 6); however, we cannot rule out the possibility that insulin activates IGF-I receptors since a relatively high concentration of insulin was required to stimulate MHC expression within 24 h (Fig. 5). Surprisingly, however, we found the potency of insulin's myogenic action to also be remarkably affected by extracellular glucose levels and that insulin exerts its potent myogenic effect only in the presence of relatively high levels of glucose, whereas its potency is significantly compromised in the absence of sufficient glucose (Fig. 5), perhaps due to massive increases in SIRT1 and FoxO3a, serving as negative regulators of this process, which are induced by insulin treatment under LG conditions (Figs. 4 and 6). Taken together, these results reveal an important interplay between glucose availability and insulin in the regulation of myogenesis, which is achieved, at least partially, through alterations in the cellular contents and nuclear abundances of SIRT1 and FoxO3a. Our data also document opposing effects of insulin, depending on glucose availability and thereby on the regulation of SIRT1 and FoxO3a amounts in differentiating C_2C_{12} myotubes (Fig. 6*A*). Since insulin/IGFs often display opposite biological effects, e.g., proliferation and differentiation, depending on conditions and circumstances (8, 11, 28, 30), our data presented herein provide a conceptual framework for understanding the mode of insulin actions (and presumably those of IGFs) by providing evidence that insulin's myogenic action is profoundly influenced by glucose availability mediated through regulation of SIRT1 and FoxO3a, both of which have been shown to be directly involved in the determination of cellular fates, including proliferation, differentiation, and senescence, in various cell types (1, 4, 5, 44, 50, 51).

Effects of ambient glucose levels on regulation of SIRT1 and FoxOs during myogenesis. A recent report revealed an important SIRT1 role in myogenesis by showing that overexpression of SIRT1 inhibited myogenesis, whereas either siRNA-mediated suppression of SIRT1 or sirtinol enhanced it by altering the acetylation states of MyoD and the histone acetylase p300/CBP (14). Although the SIRT1 expression level was shown to be slightly decreased upon differentiation of C_2C_{12}, the authors focused primarily on the importance of the regulation of its enzymatic activity rather than the expression level of SIRT1. In the present study, we found that SIRT1 expression is influenced by glucose levels and that SIRT1 abundance is significantly reduced in C_2C_{12} myotubes differentiated under HG conditions, a culture condition obviously potentiating myogenesis (Fig. 1). In addition, 24 h exposure of differentiating C_2C_{12} myotubes to HG (*days 5–6*) was also sufficient to decrease SIRT1 abundance (Fig. 2C), which apparently contributed to the potentiation of myogenesis as assessed by MHC expression levels (Fig. 5). Although acute redistribution was not observed with either glucose or insulin in the present study (Fig. 2B), recent reports revealed the existence of a nucleocytoplasmic shuttling mechanism for SIRT1 (24, 50). Thus, our data strongly suggest that SIRT1 abundance and its localization, being sensitively influenced by ambient glucose levels, are also directly involved in the regulation of myogenesis as a prerequisite for regulating its enzymatic activity at suitable

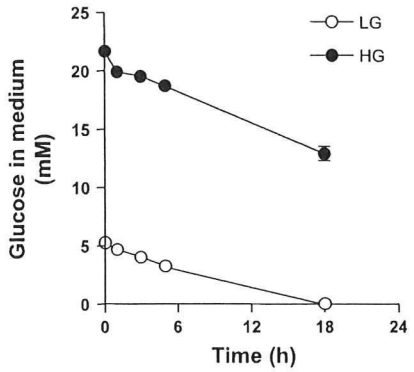

Fig. 7. Glucose consumption by C_2C_{12} myotubes. C_2C_{12} myoblasts were differentiated into myotubes for 6 days. Media were then switched to fresh medium containing LG (●) or HG (○), and glucose concentrations were measured at the indicated time.

site(s). Consistent with this idea, a recent report demonstrated SIRT1 transcription to be regulated by metabolic states via the HIC1:CtBP corepressor complex (55). These changes in SIRT1 abundance in skeletal muscle cells may contribute not only to myogenesis but also to metabolic adaptations during glucose deprivation, such as regulation of mitochondrial gene expression and fatty acid utilization (17, 29).

Similar to what was observed in SIRT1 regulation, we found decreases in both the cellular and the nuclear abundance of FoxO3a to also be coupled to the potentiation of myogenesis, which can be induced under HG conditions (Figs. 1 and 3). These findings are consistent with a previous report showing that short interfering RNA-mediated suppression of FoxOs enhanced myogenesis, whereas its overexpression inhibited differentiation (21). Although the importance of nucleocytoplasmic shuttling of FoxOs by posttranslational modifications, such as the interplay between the Akt-mediated phosphorylation and the SIRT1-mediated deacetylation in response to growth factors and oxidative stress, is well established (3, 4), acute redistribution of FoxO3a was not detected with changes in the ambient glucose level (Fig. 3*B*), whereas its nuclear exclusion was rapidly induced by insulin, as previously reported (49). Since C_2C_{12} myocytes also express other FoxO family transcription factors, including FoxO1 and FoxO4, in addition to FoxO3a (21), our data at this stage cannot address the magnitude of the FoxO3a contribution to myogenic inhibitory action. However, our present data support previous reports showing that both SIRT1 and FoxO3a serve as negative myogenic regulators (14, 21) and also provide evidence supporting the important participation of these proteins in the process of myogenesis achieved through the regulation of their amounts and subcellular localizations. As discussed below, the physiological importance of glucose-dependent alterations in cellular SIRT1 and FoxO3a abundance in myogenesis further underscores our striking finding that insulin exerts distinct effects regulating the abundances of these proteins depending on glucose availability, which is tightly coupled with myogenic differentiation status (Fig. 4 and Fig. 5).

Interplay between ambient glucose and insulin in regulation of SIRT1 and FoxO3a and its involvement in myogenesis. In the present study, we found that the effects of ambient glucose levels can be exerted within 24 h, according to the cellular abundances of both SIRT1 and FoxO3a (Figs. 2 and 3), in differentiating C_2C_{12} myotubes. Similarly, the drastic changes in SIRT1 and FoxO abundances in various tissues, including skeletal muscle, have been reported for in vivo experiments showing that starvation increases SIRT1 and FoxOs, which are resuppressed by refeeding within 24 h (15, 16, 38, 45). In this regard, we observed that the extracellular glucose concentration falls to less than 0.5 mM after a 24-h incubation when differentiating C_2C_{12} cells are cultured in LG-DMEM (Fig. 7), even though DMEM containing 5 mM glucose (LG) is a conventional medium routinely utilized to maintain various cell types. This is probably because myotubes are postmitotic multinuclear cells that consume vast amounts of glucose as an energy source. Consequently, the cells cultured under LG conditions were perhaps experiencing an environment similar to the condition of glucose starvation, of varying degrees, during the 24-h incubation, even though the LG media were replaced daily, whereas when cells were cultured under HG conditions they were continually exposed to pathophysiologically high levels of glucose for 24 h (Fig. 7). Hence, our observations indicate that these gross culture environments, including the consequences of glucose consumption and/or exhaustion, not just the initial glucose concentration, apparently contribute to regulating SIRT1 and FoxO3a, which is in turn responsible for the modulation of myogenesis during the 24-h incubation.

One of the most intriguing observations is that insulin remarkably increases the cellular contents of both SIRT1 and FoxO3a under only LG conditions (Fig. 4*A*, *lanes 1–6*), whereas insulin completely fails to increase FoxO3a, instead decreasing the SIRT1 amount in the presence of HG (Fig. 4*A*, *lanes 7–12*). Moreover, our most striking finding is that insulin is unable to exert its myogenic action under LG conditions (Fig. 5*A*, *lanes 1–5*), whereas its potency is maximized under HG conditions, as assessed by MHC expression levels (Fig. 5*A*, *lanes 6–10*). Although it is well established that insulin and IGFs serve as potent myogenic stimulators (7, 12, 21), our present data reveal insulin's myogenic action to be significantly influenced by glucose availability. In addition, our data strongly suggest that the insulin-induced massive accumulations of these negative myogenic transcriptional regulators, SIRT1 and FoxO3a, provoked under LG conditions in differentiating C_2C_{12} myotubes counteract the myogenic stimulatory potency that insulin intrinsically possesses.

The important functional interrelationships between SIRT1 and FoxOs have been established in various organisms (18), and SIRT1 and FoxOs, including FoxO3a, have been shown to physically interact with each other to regulate their functions in a wide array of cell types (4, 10, 36). Thus, although either SIRT1 or FoxO3a alone is reportedly able to interfere with the process of myogenesis (21), it is likely that SIRT1 and FoxO3a are cooperatively involved in this interference, properly responding to alterations of culture circumstances such as glucose availability and the presence of insulin. In an attempt to evaluate the contribution of the myogenic inhibitory actions of these proteins, we utilized sirtinol to eliminate the deacetylase activity of SIRT1 and found that, although the poor differentiation state under LG conditions is significantly restored within 24 h by sirtinol (Fig. 6*C*, *bottom, lanes 1–4*), as previously reported (14), the sirtinol-dependent restoration of increased MHC expression is completely abolished in the presence of insulin (*lanes 5–8*). These data not only further confirm the opposing actions of insulin, i.e., that insulin can serve as a negative, rather than a positive, myogenic factor when glucose availability is low, but also suggest that the reduction of SIRT1 enzymatic activity alone might be insufficient to overcome the poor differentiation status in the presence of insulin, a condition under which FoxO3a is remarkably increased (Fig. 6*C*, *middle, lanes 5–8*). Thus, the considerably augmented FoxO3a may still be functional to some extent even in the presence of insulin during a 24-h incubation, which perhaps contributes to interference with the promotion of myogenesis. Moreover, since both FoxO1 and FoxO3a have been shown to increase the expressions of the ubiquitin ligases MAFbx and MuRF1, responsible for muscle atrophy via increased protein degradation (46, 49), the increased FoxO3a may also participate in the stimulation of protein degradation governed by these FoxO-inducible ubiquitin ligases. In any case, together with previous studies showing that overexpression of FoxOs results in reduced muscle mass in transgenic

mice (27) and also retards myogenesis (21), our present data suggest that the massively increased FoxO3a plays a pivotal role in exerting the inhibitory actions of insulin, at least under these experimental conditions.

Another interesting observation presented in this study is that the opposing actions of insulin depending on ambient glucose levels were both completely abolished by LY-294002 (Fig. 6*A*) or rapamycin (Fig. 6*B*). These results indicate crucial involvements of the PI 3-kinase and mTOR activities stimulated by insulin in exerting insulin actions on SIRT1 and FoxO3a depending on ambient glucose environments (Fig. 6), although the insulin-induced decrease in FoxO3a under HG conditions is not apparent due to its undetectable expression (Fig. 6, *A* and *B*, *middle, lanes 4–6*), as was the case with that observed in SIRT1 (Fig. 6, *A* and *B*, *top, lanes 4–6*). Recently, Southgate et al. (48) showed that the elevation of FoxO1 protein levels induced the nonphosphorylated form of 4EBP1, followed by reductions in Raptor and mTOR protein amounts. Together with our finding that the opposing actions of insulin on FoxO3a protein levels, which depend upon ambient glucose concentrations, are both abolished by rapamycin (Fig. 6), it is reasonable to speculate that insulin stimulates either negative or positive feedback loops on the mTOR-FoxO axis, depending on ambient glucose levels. Future work should be directed toward increasing our understanding of the mechanisms underlying the differential effects of insulin on SIRT1 and FoxOs, depending on glucose availability to solve the mystery of how insulin/IGFs exert diverse, and in some instances opposing, biological actions.

ACKNOWLEDGMENTS

We thank Fumie Wagatsuma and Natsumi Emoto for technical assistance.

GRANTS

This work was supported by Special Coordination Funds for Promoting Science and Technology. This work was also supported in part by grants from the Ministry of Education, Culture, Sports, Science and Technology of Japan and the New Energy and Industrial Technology Development Organization (NEDO).

REFERENCES

1. **Birkenkamp KU, Essafi A, van der Vos KE, da Costa M, Hui RC, Holstege F, Koenderman L, Lam EW, Coffer PJ.** FOXO3a induces differentiation of Bcr-Abl-transformed cells through transcriptional down-regulation of Id1. *J Biol Chem* 282: 2211–2220, 2007.
2. **Blander G, Guarente L.** The Sir2 family of protein deacetylases. *Annu Rev Biochem* 73: 417–435, 2004.
3. **Brunet A, Bonni A, Zigmond MJ, Lin MZ, Juo P, Hu LS, Anderson MJ, Arden KC, Blenis J, Greenberg ME.** Akt promotes cell survival by phosphorylating and inhibiting a Forkhead transcription factor. *Cell* 96: 857–868, 1999.
4. **Brunet A, Sweeney LB, Sturgill JF, Chua KF, Greer PL, Lin Y, Tran H, Ross SE, Mostoslavsky R, Cohen HY, Hu LS, Cheng HL, Jedrychowski MP, Gygi SP, Sinclair DA, Alt FW, Greenberg ME.** Stress-dependent regulation of FOXO transcription factors by the SIRT1 deacetylase. *Science* 303: 2011–2015, 2004.
5. **Chua KF, Mostoslavsky R, Lombard DB, Pang WW, Saito S, Franco S, Kaushal D, Cheng HL, Fischer MR, Stokes N, Murphy MM, Appella E, Alt FW.** Mammalian SIRT1 limits replicative life span in response to chronic genotoxic stress. *Cell Metab* 2: 67–76, 2005.
6. **Conejo R, de Alvaro C, Benito M, Cuadrado A, Lorenzo M.** Insulin restores differentiation of Ras-transformed C2C12 myoblasts by inducing NF-kappaB through an AKT/P70S6K/p38-MAPK pathway. *Oncogene* 21: 3739–3753, 2002.
7. **Conejo R, Valverde AM, Benito M, Lorenzo M.** Insulin produces myogenesis in C2C12 myoblasts by induction of NF-kappaB and down-regulation of AP-1 activities. *J Cell Physiol* 186: 82–94, 2001.
8. **Coolican SA, Samuel DS, Ewton DZ, McWade FJ, Florini JR.** The mitogenic and myogenic actions of insulin-like growth factors utilize distinct signaling pathways. *J Biol Chem* 272: 6653–6662, 1997.
9. **Cushman SW, Goodyear LJ, Pilch PF, Ralston E, Galbo H, Ploug T, Kristiansen S, Klip A.** Molecular mechanisms involved in GLUT4 translocation in muscle during insulin and contraction stimulation. *Adv Exp Med Biol* 441: 63–71, 1998.
10. **Daitoku H, Hatta M, Matsuzaki H, Aratani S, Ohshima T, Miyagishi M, Nakajima T, Fukamizu A.** Silent information regulator 2 potentiates Foxo1-mediated transcription through its deacetylase activity. *Proc Natl Acad Sci USA* 101: 10042–10047, 2004.
11. **Ewton DZ, Florini JR.** Effects of the somatomedins and insulin on myoblast differentiation in vitro. *Dev Biol* 86: 31–39, 1981.
12. **Florini JR, Ewton DZ, Coolican SA.** Growth hormone and the insulin-like growth factor system in myogenesis. *Endocr Rev* 17: 481–517, 1996.
13. **Fujita H, Nedachi T, Kanzaki M.** Accelerated de novo sarcomere assembly by electric pulse stimulation in C2C12 myotubes. *Exp Cell Res* 313: 1853–1865, 2007.
14. **Fulco M, Schiltz RL, Iezzi S, King MT, Zhao P, Kashiwaya Y, Hoffman E, Veech RL, Sartorelli V.** Sir2 regulates skeletal muscle differentiation as a potential sensor of the redox state. *Mol Cell* 12: 51–62, 2003.
15. **Furuyama T, Kitayama K, Yamashita H, Mori N.** Forkhead transcription factor FOXO1 (FKHR)-dependent induction of PDK4 gene expression in skeletal muscle during energy deprivation. *Biochem J* 375: 365–371, 2003.
16. **Furuyama T, Yamashita H, Kitayama K, Higami Y, Shimokawa I, Mori N.** Effects of aging and caloric restriction on the gene expression of Foxo1, 3, and 4 (FKHR, FKHRL1, and AFX) in the rat skeletal muscles. *Microsc Res Tech* 59: 331–334, 2002.
17. **Gerhart-Hines Z, Rodgers JT, Bare O, Lerin C, Kim SH, Mostoslavsky R, Alt FW, Wu Z, Puigserver P.** Metabolic control of muscle mitochondrial function and fatty acid oxidation through SIRT1/PGC-1alpha. *EMBO J* 26: 1913–1923, 2007.
18. **Giannakou ME, Partridge L.** The interaction between FOXO and SIRT1: tipping the balance towards survival. *Trends Cell Biol* 14: 408–412, 2004.
19. **Gotta M, Strahl-Bolsinger S, Renauld H, Laroche T, Kennedy BK, Grunstein M, Gasser SM.** Localization of Sir2p: the nucleolus as a compartment for silent information regulators. *EMBO J* 16: 3243–3255, 1997.
20. **Grozinger CM, Chao ED, Blackwell HE, Moazed D, Schreiber SL.** Identification of a class of small molecule inhibitors of the sirtuin family of NAD-dependent deacetylases by phenotypic screening. *J Biol Chem* 276: 38837–38843, 2001.
21. **Hribal ML, Nakae J, Kitamura T, Shutter JR, Accili D.** Regulation of insulin-like growth factor-dependent myoblast differentiation by Foxo forkhead transcription factors. *J Cell Biol* 162: 535–541, 2003.
22. **Jiang BH, Aoki M, Zheng JZ, Li J, Vogt PK.** Myogenic signaling of phosphatidylinositol 3-kinase requires the serine-threonine kinase Akt/protein kinase B. *Proc Natl Acad Sci USA* 96: 2077–2081, 1999.
23. **Jiang BH, Zheng JZ, Vogt PK.** An essential role of phosphatidylinositol 3-kinase in myogenic differentiation. *Proc Natl Acad Sci USA* 95: 14179–14183, 1998.
24. **Jin Q, Yan T, Ge X, Sun C, Shi X, Zhai Q.** Cytoplasm-localized SIRT1 enhances apoptosis. *J Cell Physiol* 213: 88–97, 2007.
25. **Kaliman P, Canicio J, Shepherd PR, Beeton CA, Testar X, Palacin M, Zorzano A.** Insulin-like growth factors require phosphatidylinositol 3-kinase to signal myogenesis: dominant negative p85 expression blocks differentiation of L6E9 muscle cells. *Mol Endocrinol* 12: 66–77, 1998.
26. **Kaliman P, Vinals F, Testar X, Palacin M, Zorzano A.** Phosphatidylinositol 3-kinase inhibitors block differentiation of skeletal muscle cells. *J Biol Chem* 271: 19146–19151, 1996.
27. **Kamei Y, Miura S, Suzuki M, Kai Y, Mizukami J, Taniguchi T, Mochida K, Hata T, Matsuda J, Aburatani H, Nishino I, Ezaki O.** Skeletal muscle FOXO1 (FKHR) transgenic mice have less skeletal muscle mass, down-regulated type I (slow twitch/red muscle) fiber genes, and impaired glycemic control. *J Biol Chem* 279: 41114–41123, 2004.
28. **Kanzaki M, Hattori M, Kojima I.** Growth or differentiation: determination by FSH of the action of insulin-like growth factor-I in cultured rat granulosa cells. *Endocr J* 43: 15–23., 1996.
29. **Lagouge M, Argmann C, Gerhart-Hines Z, Meziane H, Lerin C, Daussin F, Messadeq N, Milne J, Lambert P, Elliott P, Geny B, Laakso M, Puigserver P, Auwerx J.** Resveratrol improves mitochondrial

function and protects against metabolic disease by activating SIRT1 and PGC-1alpha. *Cell* 127: 1109–1122, 2006.
30. **Lorenzo M, Valverde AM, Teruel T, Benito M.** IGF-I is a mitogen involved in differentiation-related gene expression in fetal rat brown adipocytes. *J Cell Biol* 123: 1567–1575, 1993.
31. **Lu J, McKinsey TA, Zhang CL, Olson EN.** Regulation of skeletal myogenesis by association of the MEF2 transcription factor with class II histone deacetylases. *Mol Cell* 6: 233–244, 2000.
32. **Luo J, Nikolaev AY, Imai S, Chen D, Su F, Shiloh A, Guarente L, Gu W.** Negative control of p53 by Sir2alpha promotes cell survival under stress. *Cell* 107: 137–148, 2001.
33. **McKinsey TA, Zhang CL, Lu J, Olson EN.** Signal-dependent nuclear export of a histone deacetylase regulates muscle differentiation. *Nature* 408: 106–111, 2000.
34. **Michishita E, Park JY, Burneskis JM, Barrett JC, Horikawa I.** Evolutionarily conserved and nonconserved cellular localizations and functions of human SIRT proteins. *Mol Biol Cell* 16: 4623–4635, 2005.
35. **Molkentin JD, Black BL, Martin JF, Olson EN.** Cooperative activation of muscle gene expression by MEF2 and myogenic bHLH proteins. *Cell* 83: 1125–1136, 1995.
36. **Motta MC, Divecha N, Lemieux M, Kamel C, Chen D, Gu W, Bultsma Y, McBurney M, Guarente L.** Mammalian SIRT1 represses forkhead transcription factors. *Cell* 116: 551–563, 2004.
37. **Nedachi T, Kanzaki M.** Regulation of glucose transporters by insulin and extracellular glucose in C_2C_{12} myotubes. *Am J Physiol Endocrinol Metab* 291: E817–E828, 2006.
38. **Nemoto S, Fergusson MM, Finkel T.** Nutrient availability regulates SIRT1 through a forkhead-dependent pathway. *Science* 306: 2105–2108, 2004.
39. **Park IH, Chen J.** Mammalian target of rapamycin (mTOR) signaling is required for a late-stage fusion process during skeletal myotube maturation. *J Biol Chem* 280: 32009–32017, 2005.
40. **Picard F, Kurtev M, Chung N, Topark-Ngarm A, Senawong T, Machado De Oliveira R, Leid M, McBurney MW, Guarente L.** Sirt1 promotes fat mobilization in white adipocytes by repressing PPAR-gamma. *Nature* 429: 771–776, 2004.
41. **Pinset C, Garcia A, Rousse S, Dubois C, Montarras D.** Wortmannin inhibits IGF-dependent differentiation in the mouse myogenic cell line C2. *C R Acad Sci III* 320: 367–374, 1997.
42. **Pownall ME, Gustafsson MK, Emerson CP Jr.** Myogenic regulatory factors and the specification of muscle progenitors in vertebrate embryos. *Annu Rev Cell Dev Biol* 18: 747–783, 2002.
43. **Puri PL, Iezzi S, Stiegler P, Chen TT, Schiltz RL, Muscat GE, Giordano A, Kedes L, Wang JY, Sartorelli V.** Class I histone deacetylases sequentially interact with MyoD and pRb during skeletal myogenesis. *Mol Cell* 8: 885–897, 2001.
44. **Qiao L, Shao J.** SIRT1 regulates adiponectin gene expression through Foxo1-C/enhancer-binding protein alpha transcriptional complex. *J Biol Chem* 281: 39915–39924, 2006.
45. **Rodgers JT, Lerin C, Haas W, Gygi SP, Spiegelman BM, Puigserver P.** Nutrient control of glucose homeostasis through a complex of PGC-1alpha and SIRT1. *Nature* 434: 113–118, 2005.
46. **Sandri M, Sandri C, Gilbert A, Skurk C, Calabria E, Picard A, Walsh K, Schiaffino S, Lecker SH, Goldberg AL.** Foxo transcription factors induce the atrophy-related ubiquitin ligase atrogin-1 and cause skeletal muscle atrophy. *Cell* 117: 399–412, 2004.
47. **Shu L, Zhang X, Houghton PJ.** Myogenic differentiation is dependent on both the kinase function and the N-terminal sequence of mammalian target of rapamycin. *J Biol Chem* 277: 16726–16732, 2002.
48. **Southgate RJ, Neill B, Prelovsek O, El-Osta A, Kamei Y, Miura S, Ezaki O, McLoughlin TJ, Zhang W, Unterman TG, Febbraio MA.** FOXO1 regulates the expression of 4E-BP1 and inhibits mTOR signaling in mammalian skeletal muscle. *J Biol Chem* 282: 21176–21186, 2007.
49. **Stitt TN, Drujan D, Clarke BA, Panaro F, Timofeyva Y, Kline WO, Gonzalez M, Yancopoulos GD, Glass DJ.** The IGF-1/PI3K/Akt pathway prevents expression of muscle atrophy-induced ubiquitin ligases by inhibiting FOXO transcription factors. *Mol Cell* 14: 395–403, 2004.
50. **Tanno M, Sakamoto J, Miura T, Shimamoto K, Horio Y.** Nucleocytoplasmic shuttling of the NAD+-dependent histone deacetylase SIRT1. *J Biol Chem* 282: 6823–6832, 2007.
51. **van der Horst A, Tertoolen LG, de Vries-Smits LM, Frye RA, Medema RH, Burgering BM.** FOXO4 is acetylated upon peroxide stress and deacetylated by the longevity protein hSir2 (SIRT1). *J Biol Chem* 279: 28873–28879, 2004.
52. **Wan X, Harkavy B, Shen N, Grohar P, Helman LJ.** Rapamycin induces feedback activation of Akt signaling through an IGF-1R-dependent mechanism. *Oncogene* 26: 1932–1940, 2007.
53. **Xu Q, Wu Z.** The insulin-like growth factor-phosphatidylinositol 3-kinase-Akt signaling pathway regulates myogenin expression in normal myogenic cells but not in rhabdomyosarcoma-derived RD cells. *J Biol Chem* 275: 36750–36757, 2000.
54. **Yaffe D, Saxel O.** Serial passaging and differentiation of myogenic cells isolated from dystrophic mouse muscle. *Nature* 270: 725–727, 1977.
55. **Zhang Q, Wang SY, Fleuriel C, Leprince D, Rocheleau JV, Piston DW, Goodman RH.** Metabolic regulation of SIRT1 transcription via a HIC1:CtBP corepressor complex. *Proc Natl Acad Sci USA* 104: 829–833, 2007.

THE JOURNAL OF BIOLOGICAL CHEMISTRY VOL. 283, NO. 15, pp. 10208–10220, April 11, 2008

Functional Role of Sortilin in Myogenesis and Development of Insulin-responsive Glucose Transport System in C2C12 Myocytes*

Received for publication, December 31, 2007 Published, JBC Papers in Press, February 7, 2008, DOI 10.1074/jbc.M710604200

Miyako Ariga[‡§¶1], **Taku Nedachi**[§], **Hideki Katagiri**[‡¶], **and Makoto Kanzaki**[§2]

From the [‡]*21st Century COE program Comprehensive Research and Education Center for Planning of Drug Development and Clinical Evaluation, Graduate School of Pharmaceutical Sciences, Tohoku University, Sendai 980-8575, the* [§]*Division of Biomaterials, Biomedical Engineering Research Organization, Tohoku University, 2-1 Seiryo-machi, Aoba-ku, Sendai 980-8575, and the* [¶]*Division of Advanced Therapeutics for Metabolic Diseases, Center for Translational and Advanced Animal Research, Tohoku University Graduate School of Medicine, Sendai 980-8575, Japan*

Sortilin has been implicated in the formation of insulin-responsive GLUT4 storage vesicles in adipocytes by regulating sorting events between the *trans*-Golgi-network and endosomes. We herein show that sortilin serves as a potent myogenic differentiation stimulator for C2C12 myocytes by cooperatively functioning with p75NTR, which subsequently further contributes to development of the insulin-responsive glucose transport system in C2C12 myotubes. Sortilin expression was up-regulated upon C2C12 differentiation, and overexpression of sortilin in C2C12 cells significantly stimulated myogenic differentiation, a response that was completely abolished by either anti-p75NTR- or anti-nerve growth factor (NGF)-neutralizing antibodies. Importantly, small interference RNA-mediated suppression of endogenous sortilin significantly inhibited C2C12 differentiation, indicating the physiological significance of sortilin expression in the process of myogenesis. Although sortilin overexpression in C2C12 myotubes improved insulin-induced 2-deoxyglucose uptake, as previously reported, this effect apparently resulted from a decrease in the cellular content of GLUT1 and an increase in GLUT4 via differentiation-dependent alterations at both the gene transcriptional and the post-translational level. In addition, cellular contents of Ubc9 and SUMO-modified proteins appeared to be increased by sortilin overexpression. Taken together, these data demonstrate that sortilin is involved not only in development of the insulin-responsive glucose transport system in myocytes, but is also directly involved in muscle differentiation via modulation of proNGF-p75NTR.

One of the major physiological roles of insulin is the control of postprandial blood glucose levels, and skeletal muscle is the primary tissue responsible for the bulk (70–80%) of insulin-stimulated postprandial glucose disposal (1, 2). The effect of insulin on overall glucose disposal is primarily achieved via stimulation of glucose uptake into insulin-target tissues, and defects in this insulin action in skeletal muscle contribute to development of the insulin resistance which is characteristic of type 2 diabetes (3).

In skeletal muscle, glucose transport is regulated by a facilitative glucose transport system involving at least two members of the glucose transporter family, GLUT1 and GLUT4 (4), and their expression levels are strictly regulated during myocyte differentiation (5, 6). GLUT1 is targeted predominantly to the sarcolemma (muscle plasma membrane) and is therefore implicated in the regulation of basal glucose transport, although a marked reduction in GLUT1 expression occurs during muscle differentiation (5, 6). In contrast, expression of the insulin-responsive glucose transporter GLUT4 is remarkably up-regulated upon muscle differentiation, and GLUT4 protein is predominantly localized in intracellular tubulo-vesicular elements under basal conditions (7, 8), while insulin stimulates the translocation of GLUT4 from intracellular storage compartments to the cell surface, resulting in the insulin-responsive augmentation of glucose uptake (9). Thus, differentiation-dependent changes in the amount and composition of these GLUT proteins, especially the increase in cellular GLUT4 content, contribute to development of the insulin-responsive glucose transport system in myocytes and adipocytes (5, 10). However, GLUT4 expression is not the only factor responsible for conferring the insulin-stimulated glucose uptake function in these insulin-responsive cells, because ectopic expression of GLUT4 in other cell types such as fibroblasts is insufficient to generate an insulin-stimulated glucose transport system (11, 12).

Recent studies using adipocytes have revealed that one of the additional factors prerequisite for higher insulin responsiveness is a signaling cascade developed during the course of adipocyte differentiation that is absent in pre-adipocytes (13, 14). In addition to differentiation-dependent establishment of this signaling cascade, Kandror and colleagues (15, 16) recently reported that sortilin, a type I transmembrane glycoprotein, which is implicated in the sorting of Vps10p-interacting proteins between the *trans*-Golgi network, plasma membrane, and lysosomes, serves as another important factor that promotes development of the insulin-induced glucose transport system

* This work was supported in part by grants from the New Energy and Industrial Technology Development Organization and the Ministry of Education, Science, Sports and Culture of Japan. The costs of publication of this article were defrayed in part by the payment of page charges. This article must therefore be hereby marked "*advertisement*" in accordance with 18 U.S.C. Section 1734 solely to indicate this fact.

[1] Supported by Research Fellowships of the Japan Society for the Promotion of Science for Young Scientists.

[2] Supported by Special Coordinated Funds for Promoting Science and Technology. To whom correspondence should be addressed: Tel.: 81-22-717-7581; Fax: 81-22-717-7578; E-mail: kanzakimakoto@mac.com.

by producing insulin-responsive GLUT4 storage vesicles. They found that fibroblasts ectopically expressing both sortilin and GLUT4 display significantly augmented glucose uptake in response to insulin stimulation (12). Although it has already been reported that sortilin is expressed in muscle (17, 18), at present the functional role of sortilin in muscle is entirely unknown, although muscle is the tissue in which the insulin effect on postprandial glucose disposal is quantitatively most important.

Sortilin was originally purified from human brain extracts using receptor-associated protein affinity chromatography (17) and was also identified as a major component of GLUT4-containing vesicles from rat adipocytes (18, 19). Sortilin has a Vps10p domain in its luminal region at the N terminus and therefore belongs to the mammalian VPS10p family of sorting receptors. The intraluminal domain of sortilin was shown to interact with a wide array of proteins, including an unprocessed form of nerve growth factor (proNGF),[3] neurotensin, lipoprotein lipase, precursor of brain-derived neurotrophic factor (BDNF), and prosaposin, as well as receptor-associated protein (16, 17, 20–23). Therefore, sortilin functions not only to direct the intracellular movements of such newly synthesized interacting proteins but also functions as a receptor for these proteins once sortilin is exposed to the cell surface plasma membrane. Nevertheless, the cytoplasmic tail of sortilin does not possess a domain enabling it to directly activate the intracellular signaling cascade (24). Recent studies have, however, revealed that sortilin forms a complex with proNGF and p75NTR, a low affinity NGF receptor, and triggers p75NTR signaling cascades leading to various cellular responses, including differentiation, survival, and apoptosis (22, 25). Interestingly, genes encoding precursors of NGF and BDNF, and their common low affinity receptor p75NTR, were shown to be expressed in C2C12 myoblasts (26). In addition, several lines of evidence indicate that NGF affects myogenic differentiation and muscle development in an autocrine fashion via p75NTR (26–28).

In the present study, we explored the functional roles of sortilin in muscle by using the skeletal muscle cell line C2C12. We herein report sortilin to be a potent differentiation stimulator functioning cooperatively with p75NTR, which subsequently further contributes to development of the insulin responsive glucose transport system in C2C12 cells. We present compelling evidence that sortilin is involved not only in generating insulin-responsive GLUT4 storage vesicles but also in elaborating an entire glucose transport system exhibiting much higher insulin responsiveness via regulation of the processes of myogenesis, including expressions of GLUT proteins and perhaps various other proteins involved in the development of insulin responsiveness. Thus, our results provide new insights into the functional roles of sortilin in myogenesis and in development of the insulin-responsive glucose transport system in myocytes.

[3] The abbreviations used are: proNGF, unprocessed form of nerve growth factor; NGF, nerve growth factor; p75NTR, p75 neurotrophin receptor; Vps, vacuolar protein sorting; GGA, Golgi-localizing γ-adaptin ear homology domain, ARF-binding proteins; ARF, ADP-ribosylation factor; siRNA, small interfering RNA; SUMO, small ubiquitin-related modifier; BDNF, brain-derived neurotrophic factor; MHC, myosin heavy chain; DMEM, Dulbecco's modified Eagle's medium; BSA, bovine serum albumin; ECFP, enhanced cyan fluorescent protein; PBS, phosphate-buffered saline; Ab, antibody.

EXPERIMENTAL PROCEDURES

Materials—We obtained 2-deoxy-[^{3}H]glucose (37.2 Ci/mmol) from PerkinElmer Life Sciences. The Western blot detection kit (West super femto detection reagents) was from Pierce. Dulbecco's Modified Eagle Medium (DMEM), penicillin/streptomycin and Trypsin-EDTA were purchased from Sigma. Cell culture equipment was from BD Biosciences (San Jose, CA). Calf serum and fetal bovine serum were obtained from BioWest (Nuaille, France). Immobilon-P was from Millipore Corp. (Bedford, MA). Bovine serum albumin (BSA) was purchased from Wako (Osaka, Japan). Antibodies against sortilin, p115, syntaxin 6, Ubc9, and SUMO-modified protein 1 (GMP1) were purchased from BD Biosciences. Anti-sortilin antibody obtained from Abcam (Cambridge, UK) was used for immunofluorescent analyses. Antibodies against cation-independent mannose 6-phosphate/insulin-like growth factor-2 receptor, insulin receptor β-subunit, and c-Myc (9E10) were purchased from Santa Cruz Biotechnology (Santa Cruz, CA). Anti-myosin heavy chain (MHC) (MF20), anti-myogenin (F5D), anti-troponin T (CT3), and anti-titin (9D10) antibodies were obtained from Iowa Hybridoma Bank (University of Iowa, Iowa City, IA). Anti-sarcomeric α-actinin (EA-53) and anti-β-actin (A-2066) antibodies were purchased from Sigma. Anti-GLUT1 antibody was purchased from Chemicon International Inc. (Temecula, CA). Anti-p75NTR antibody (ME20.4) was obtained from Abcam. Anti-GLUT4 antibody was a generous gift from Dr. H. Shibata (Gunma University, Maebashi, Japan) (29). Fluorescence-conjugated secondary antibodies were obtained from Invitrogen. Unless otherwise noted, all chemicals were of the purest grade available from Sigma Chemicals.

Cell Culture—Myoblasts from the mouse skeletal muscle cell line C2C12 (30) were maintained in DMEM supplemented with 10% fetal bovine serum, 30 mg/ml penicillin, and 100 mg/ml streptomycin (growth medium) at 37 °C under a 5% CO_2 atmosphere. For biochemical study, cells were grown on 6-well plates (BD Biosciences) at a density of 3×10^4 cells/well in 3 ml of growth medium. Three days after plating, the cells had reached ~80–90% confluence (Day 0). Differentiation was then induced by switching the growth medium to DMEM supplemented with 2% calf serum, 30 μg/ml penicillin, and 100 μg/ml streptomycin (differentiation medium). The differentiation medium was changed every 24 h. For the immunofluorescent staining study, cells were grown on 22-mm glass coverslips (Matsunami C022221, Osaka, Japan) in 6-well plates.

Generation of C2C12 Cells Expressing Sortilin—Human sortilin cDNA was inserted into a pMXs retroviral vector, which is generated by modifying the pBABE retroviral vector (31). The pMXs-sortilin or pMXs (control) was transfected into Plat E cells using FuGENE 6 transfection reagents (Roche Applied Science, Indianapolis, IN), and high titer retroviral supernatants were obtained. C2C12 myoblasts were infected with the generated retrovirus in growth medium containing 10 μg/ml Polybrene. Two days after infection, positive selection was performed in the presence of 5 μg/ml puromycin, and 20 individual clones were isolated. The sortilin expression level in

each clone was analyzed by Western blotting as described below.

Adenoviral Expression of Myc-GLUT4-ECFP in C2C12 Cells—An adenoviral technique was used to express rat GLUT4, possessing the c-Myc epitope tag in the first extracellular loop and enhanced cyan fluorescent protein (ECFP) at the C terminus. Briefly, established exofacial-Myc-GLUT4-ECFP cDNA (32) was inserted into adenoviral vector pHMCA5, generously provided by Dr. H. Mizuguchi (33, 34). The high titer viruses were produced by transfection of pHMCA5-Myc-GLUT4-ECFP or empty vector into 293 cells using FuGENE 6 transfection reagents (Roche Applied Science). Viral stocks of $5–50 \times 10^7$ plaque-forming units/ml were prepared in serum-free DMEM and frozen at −80 °C. The next day the medium was changed, and incubation was continued for another 24 h. Then, 2-deoxy[^{3}H]glucose and Myc antibody uptake assays were performed as described below. Expression of Myc-GLUT4-ECFP was confirmed by Western blotting and immunofluorescent staining.

Western Blot Analysis—The expression levels of each protein were analyzed by Western blotting. In brief, cells were lysed with NET buffer (50 mM Tris-HCl, pH 7.4, 150 mM NaCl, 1 mM EDTA, 1% Triton X-100, 0.1% SDS, 100 units/ml aprotinin, 1 mM phenylmethylsulfonyl fluoride, 5 μg/ml leupeptin, and 5 μg/ml pepstatin A). The extracts were centrifuged at 13,000 × *g* for 10 min at 4 °C to remove insoluble materials. The protein concentrations of supernatants were determined, and 3× Laemmli sample buffer was added to achieve a 1× final concentration. From 50 to 100 μg of total protein was subjected to 7.5–10% SDS-PAGE (1:30, bis:acrylamide). Proteins were transferred to a polyvinylidene difluoride membrane (Immobilon-P, Millipore Corp.), and the membranes were then blocked for 2 h at room temperature with 5% BSA in Tris-buffered saline (TBS) containing 0.1% Tween 20. Immunoblotting to detect each protein was achieved with an overnight incubation at 4 °C with 3% BSA/TBS containing either anti-sortilin antibody (1:1000), anti-myosin heavy chain (MHC) antibody (1:1000), anti-myogenin antibody (1:1000), anti-sarcomeric α-actinin antibody (1:1000), or anti-troponin T antibody (1:1000). Anti-β-actin (1:500) or anti-insulin receptor β-subunit (1:1000) antibodies were used as a loading control. Specific total proteins were visualized after subsequent incubation with a 1:5000 dilution of anti-mouse or anti-rabbit IgG conjugated to horseradish peroxidase and a SuperSignal Chemiluminescence detection procedure (Pierce). Protein concentrations were determined using a bicinchoninic acid (BCA) protein assay kit (Pierce). Three independent experiments were performed for each condition.

2-Deoxyglucose Uptake Assay—A 2-deoxy[^{3}H]glucose uptake assay was performed as previously described (35). Briefly, cells were starved in serum-free DMEM for 4 h, and then washed with Krebs-Ringer phosphate HEPES buffer (KRPH buffer; 10 mM phosphate buffer, pH 7.4, 1 mM $MgSO_4$, 1 mM $CaCl_2$, 136 mM NaCl, 4.7 mM KCl, 10 mM HEPES (pH 7.6)). The serum-starved cells were incubated without or with 100 nM insulin for 60 min in KRPH buffer and then chilled on ice. After washing with ice-cold KRPH buffer, glucose transport was determined by addition of 2-deoxy[^{3}H]glucose (PerkinElmer Life Sciences, 0.1 mM, 0.5 μCi/ml). After 4 min of incubation with the KRPH buffer containing 2-deoxy[^{3}H]glucose, the reaction was stopped by adding phosphate-buffered saline (PBS) containing 10 μM cytochalasin B (Sigma), and the cells were washed three times with ice-cold PBS. The cells were then lysed in 0.2 N NaOH solution, and 2-deoxy[^{3}H]glucose uptake was assessed by scintillation counting. 20 μM cytochalasin B were added to the assay buffer for the measurement of nonspecific background. Specific uptake, *i.e.* the background subtracted from the total uptake, was obtained. The protein content was determined in each experiment with a BCA protein assay kit. Data are presented as picomoles of 2-deoxy[^{3}H]glucose per milligram protein per minute. For each experiment, at least three assays were performed under each condition, and each experiment was repeated at least three times.

Anti-Myc Antibody Uptake Assay—For the measurement of insulin-induced GLUT4 translocation, the C2C12 cells expressing Myc-GLUT4-ECFP were starved in serum-free DMEM for 4 h, washed three times with KRPH buffer, and then placed in a CO_2 incubator with 2 ml of KRPH buffer. Ten minutes after incubation, the cells were treated with or without 100 nM insulin in the presence of 4 μg/ml of the anti-Myc antibody for 60 min. Next, the cells were washed three times with ice-cold PBS, harvested using 1× Laemmli sample buffer without bromphenol blue and 2-mercaptoethanol (2-ME). After the protein concentration had been determined, bromphenol blue and 2-mercaptoethanol were added, denatured by incubation for 5 min at 95 °C, and subjected to Western blotting using anti-mouse IgG antibody, anti-Myc antibody, or anti-Sortilin antibody.

Immunofluorescence and Image Analysis—After experimental treatments, the cells were washed in PBS and fixed for 20 min in 2% paraformaldehyde/PBS containing 0.1% Triton X-100. The cells were washed, and then blocked in PBS containing 5% calf serum plus 1% BSA for 1 h at room temperature. Primary and secondary antibodies were used at 1:100 and 1:1000 dilutions, respectively (unless otherwise indicated), in 1% BSA/PBS, and samples were mounted on glass slides with Vectashield (Vector Laboratories, Burlingame, CA). Cells were imaged using a confocal fluorescence microscope (Olympus Fluoview FV-1000) with associated application program ASW Ver. 1.3 (Olympus, Tokyo, Japan). Images were then imported into Adobe Photoshop (Adobe Systems, Inc.) for processing. Myogenin-positive cells were counted within a 500-μm × 500-μm area. At least five fields were counted for each sample under 20× microscopic magnification. For all microscopic analyses, at least three independent experiments were performed for each condition.

Subcellular Fractionation of C2C12 Cells—To detect endogenous GLUT1 and GLUT4, fractionation was performed according to the method of Tortorella and Pilch (36). Briefly, cells (three 150-mm plates for each sample) were washed with PBS three times, harvested with a cell scraper, suspended in 0.25 M sucrose, 20 mM Hepes-HCl (pH 7.4), 1 mM EDTA, 1 μg/ml aprotinin, 1 μg/ml pepstatin, 1 μg/ml leupeptin, and 1 mM phenylmethylsulfonyl fluoride, then homogenized with a Teflon glass homogenizer. The homogenate was centrifuged at 600 × *g* for 10 min at 4 °C. The supernatant was centrifuged at

100,000 × *g* for 1 h to collect the pellet for the total membrane fraction. For detection of GLUT1, the total membrane fraction was lysed in 100 μl of 1× Laemmli sample buffer, and subjected to Western blotting using anti-GLUT1 antibody (1:5840). For detection of GLUT4, the total membrane fraction was lysed in 100 μl of 8 M urea, 5% SDS, and 50 mM Tris-HCl (pH 6.8). After the protein concentration had been determined as described above, dithiothreitol and bromphenol blue were added to each sample (final concentrations, 343.6 μM and 0.005%, respectively). After incubation for 30 min at 37 °C, samples were subjected to SDS-PAGE followed by immunoblotting using anti-GLUT4 antibody (1:500) (37).

Real-time Reverse Transcription-PCR—Total RNA was prepared using TRIzol reagent according to the manufacturer's instructions and was quantified using an ND-1000 spectrophotometer (NanoDrop Technologies, Wilmington, DE). Reverse transcription was carried out using the First Strand cDNA Synthesis kit for PCR from Roche Applied Science. Real-time PCR reactions were performed using the Roche LightCycler, utilizing Roche SYBR Green reagents according to the manufacturer's instructions. Amplification of PCR products was quantified during PCR by measuring fluorescence associated with binding of double-stranded DNA to the SYBR Green dye incorporated into the reaction mixture. The sequences of the oligonucleotides used to PCR-amplify the cDNAs of interest were: GLUT4 (upper primer, 5′-TGCTCTCCTGCAGCTGATT-3′; lower primer, 5′-TTCAGCTCAGCTAGTGCGTC-3′), GLUT1 (upper primer, 5′-CTTCCTGCTCATCAATCGT-3′; lower primer, 5′-AGCTCCAAGATGGTGACCTT-3′), sortilin (upper primer, 5′-AATGGTCGAGACTATGTTGTG-3′; lower primer, 5′-CCGGTACCCATTTGTTGT-3′), and Ubc9 (upper primer, 5′-GGCACAATGAACCTGATGAAC-3′; lower primer, 5′-TTGGTGGTGAGGACGGATAGT-3′). Glyceraldehyde-3-phosphate dehydrogenase was quantified as a housekeeping gene by using: upper primer 5′-GGAGAAACCTGCCAAGTATGA-3′, and lower primer 5′-GCATCGAAGGTGGAAGAGT-3′. Following an initial denaturation step of 95 °C for 1 min, 30–45 cycles of 95 °C for 10 s, 60 °C for 1 s, and 72 °C for 10 s were used for GLUT4, GLUT1, sortilin, and Ubc9. For glyceraldehyde-3-phosphate dehydrogenase, an initial denaturation step of 95 °C for 10 min, followed by 45 cycles of 95 °C for 10 s, 57.5 °C for 15 s, and 72 °C for 15 s was used.

siRNA-mediated Reduction of Sortilin in C2C12 Cells—The siRNA species purchased from Nippon EGT Co. Ltd. (Toyama, Japan) were designed to target the following cDNA sequences: scrambled, 5′-AGGGUGGGUUUGGCCAAAATT-3′; and sortilin siRNA-1, 5′-GGUGGUGUUAACAGCAGAGTT-3′; sortilin siRNA-2, 5′-CCAUUGGUGUGAAAAUCUA-3′, and sortilin siRNA-3, 5′-GGACCACAUUACUAUACCA-3′. Scramble and sortilin siRNA-1 were modified from the reference (38), and the sequences of sortilin siRNA-2 and -3 were provided by Nippon EGT Co. Ltd. 200 nmol of sortilin siRNA, or scrambled siRNA species, was introduced into C2C12 myoblasts using Oligofectamine (Invitrogen). Ninety-six hours after transfection (day 3 of differentiation), cells were harvested with NET buffer followed by SDS-PAGE and immunoblotting using anti-sortilin antibody, anti-myogenin antibody, or anti-β-actin antibody (as a control).

Measurement of GLUT Stability—Adenoviral infected WT- and sort10-C2C12 cells expressing Myc-GLUT4-ECFP were treated with 10 μg/ml cycloheximide, and the cells were then harvested with NET buffer at the indicated time intervals. Cell lysates were subjected to SDS-PAGE, followed by Western blotting analysis using anti-GLUT1 or anti-Myc antibody.

Statistical Analysis—Results are expressed as means ± S.E., and the data were analyzed by analysis of variance followed by Student's *t* test. Differences were considered to be significant at *, $p < 0.05$; **, $p < 0.01$; and ***, $p < 0.001$.

RESULTS

Sortilin Expression during Differentiation of C2C12 Cells—To investigate the physiological role of sortilin in C2C12 myocytes, we first determined changes in expression levels of sortilin during myogenesis of C2C12 cells by Western blotting (Fig. 1*A*, *upper panel*). Sortilin was undetectable in undifferentiated C2C12 myoblasts (Day 0) but was observed as a ~100-kDa protein at Day 2 of differentiation when these myoblasts were differentiated in a differentiation medium containing 5 mM glucose. The amount of sortilin then gradually increased until Day 5 and remained unchanged up to Day 8. As a control for myogenic differentiation, expression levels of myogenin (*middle panel*) and MHC (*lower panel*) were also determined. Immunofluorescent staining demonstrated sortilin containing endosomes to be located throughout the cytoplasm. Thus, colocalizations with GLUT4 (*panels a* and *b*, *red*), cation-independent mannose 6-phosphate/insulin-like growth factor-2 receptor (*panels c* and *d*, *red*), and Syntaxin 6 (*panels e* and *f*, *red*) were obvious, although the sortilin-positive endosomes were apparently devoid of p115 (*panels g* and *h*, *red*), a *cis*-Golgi marker in differentiated C2C12 myotubes.

Expression of Sortilin Induces Spontaneous Myogenic Differentiation of C2C12 Cells—To explore the functional roles of sortilin in C2C12 myocytes, we established C2C12 cells in which sortilin is stably expressed using a retroviral technique. In the process of isolating positive clones, we unexpectedly found that overexpression of sortilin in C2C12 myoblasts often resulted in spontaneous myotubular formation even in growth medium containing 10% fetal bovine serum (data not shown). Twenty clones of drug-resistant C2C12 cells were isolated, nine of which stably expressed sortilin as assessed by Western blotting analysis. All nine clones expressing detectable levels of exogenous sortilin displayed the myotubular phenotype once they reached confluence. Three independent clones expressing sortilin, two control clones expressing empty vector, and parental wild-type cells were further analyzed. As shown in Fig. 2, in growth medium, neither wild-type C2C12 (WT-C2C12) nor the control clone expressing empty vector expressed sortilin (Fig. 2*A*, *right panel*, *lanes 1* and *2*). Furthermore, neither displayed a myotubular phenotype even after reaching confluence (Fig. 2*A*, *panels a* and *b*). In sharp contrast, C2C12 clones expressing exogenous sortilin (Sort10- and Sort15-C2C12) (Fig. 2, *right panel*, *lanes 3* and *4*) underwent spontaneous differentiation as evidenced by myotube formation (Fig. 2*A*, *left panels*, *panels c* and *d*). Immunofluorescent analysis revealed that even before differentiation began Sort10-C2C12 cells already expressed various muscle differentiation markers,

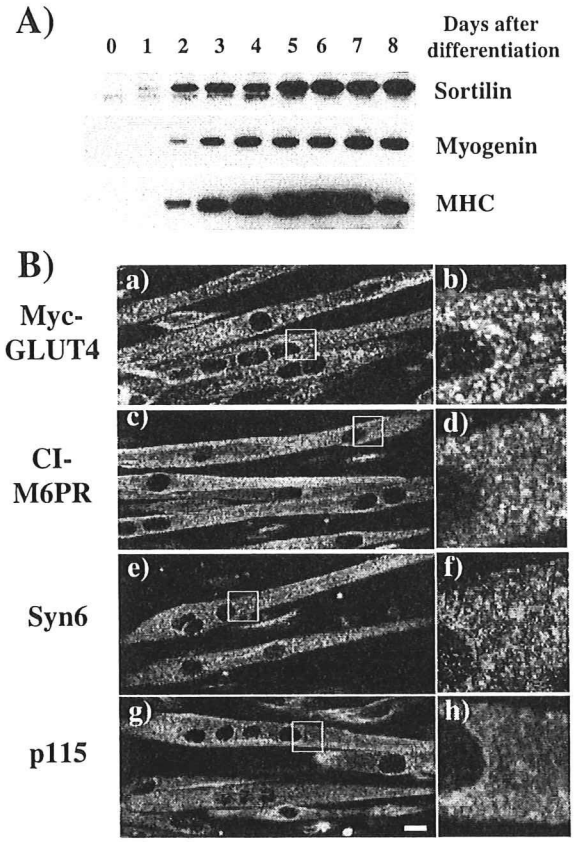

FIGURE 1. **Protein expression and subcellular localization of sortilin during C2C12 differentiation.** *A*, C2C12 myoblasts were differentiated in conventional differentiation medium (DMEM containing 5 mM glucose plus 2% calf serum). The differentiation medium was changed every 24 h. Whole cell lysates were obtained daily until day 8 of differentiation. Total protein extracts (22.5 μg/lane) were subjected to SDS-PAGE followed by Western blot analysis using anti-sortilin (*upper panel*), anti-myogenin (*middle panel*), and anti-myosin heavy chain (MHC: *lower panel*) antibodies. *B*, differentiated C2C12 myotubes (Day 6) were fixed and subjected to immunofluorescent staining using rabbit anti-sortilin antibody (*green*) with either mouse monoclonal anti-Myc (*panels a* and *b*), anti-cation-independent mannose 6-phosphate/insulin-like growth factor-2 receptor (*panels c* and *d*), anti-syntaxin 6 (*panels e* and *f*), or anti-p115 (*panels g* and *h*) antibodies (*red*). For examining co-localization between sortilin and GLUT4 (*panels a* and *b*), Myc-GLUT4-ECFP was transiently expressed by infecting C2C12 cells at Day 4 of differentiation with the adenovirus containing the Myc-GLUT4-ECFP gene and then subjecting these cells to immunofluorescent analysis at 2 days after infection (Day 6 of differentiation). Fluorescence signals were detected under confocal microscopy. The *squares* indicated in *panels a, c, d,* and *g* were magnified and are shown in the *right panels*. *Images* are representative fields of view from three independent experiments. *Scale bar* = 10 μm.

including myogenin (Fig. 2*B*, *panel d*), MHC (Fig. 2, *panel e*), and titin (Fig. 2, *panel f*), observations not made in either WT-C2C12 cells (Fig. 2*B*, *panels a–c*) or empty vector-expressing C2C12 cells (Fig. 2*B*, *panels d–f*). Essentially the same results were obtained in the other clones overexpressing sortilin, but not in other control C2C12 clone obtained by infection with empty retrovirus lacking an insert, and levels of sortilin protein in the control cells were not significantly different from those observed in the non-infected C2C12 myocytes (data not shown).

This stimulatory effect of sortilin overexpression on myogenesis was further confirmed by Western blot analysis using antibodies against various muscle differentiation marker proteins, including MHC, sarcomeric α-actinin, troponin T, and myogenin (Fig. 2*C*). Even at Day 0, Sort10-C2C12 cells already showed considerable elevations of all muscle differentiation marker proteins tested (*lane 2*), observations not made in WT-C2C12 cells (*lane 1*). At Day 4 of differentiation, all of these differentiation marker proteins were also detected in WT-C2C12 cells, although their expression levels were obviously lower in these (*lane 3*) than in Sort10-C2C12 cells (*lane 4*). At Day 7 of differentiation, most of these expressions reached comparable levels in WT-C2C12 (*lane 5*) and Sort10-C2C12 (*lane 6*) cells. Together, these data clearly demonstrate that sortilin overexpression in C2C12 myoblasts results in spontaneous myogenic differentiation once confluence is reached even under growth stimulating conditions.

Involvement of the proNGF-p75NTR Autocrine Loop in the Spontaneous Differentiation of Sortilin-overexpressing C2C12 Cells—Since recent studies have revealed direct interactions among sortilin, p75NTR, and proNGF exerting biological effects in neuronal cells (22, 25), we examined the possible involvement of proNGF and p75NTR, the existence of which in C2C12 cells was previously reported (26, 27), in the process of spontaneous differentiation induced by sortilin overexpression. To address this question, Sort10-C2C12 cells were cultured in the presence or absence of a p75NTR-neutralizing antibody that blocks p75NTR-mediated biological responses (39). The p75NTR-neutralizing antibody significantly reduced the number of Sort10-C2C12 myocytes expressing myogenin in the growth medium, whereas control mouse IgG had no such effect (Fig. 3*A*, *left panel*). In addition, essentially the same result was obtained when an NGF-neutralizing antibody that blocks both NGF and proNGF action was added to the culture instead of the p75NTR-neutralizing antibody (Fig. 3*A*, *right panel*). We also found the anti-p75NTR antibody to be very efficiently endocytosed only in C2C12 cells expressing sortilin (Fig. 3*B*, *panel d*, sortilin; *green*, mouse IgG; *red*), not in control cells expressing empty vector (Fig. 3*B*, *panel b*). No control mouse IgG was incorporated into C2C12 cells, regardless of sortilin expression during the incubation (Fig. 3*B*, *panels a* and *c*). This observation suggests that sortilin overexpression may facilitate complex formation with p75NTR, leading to efficient incorporation of the anti-p75NTR antibody. These data indicate that the stimulatory effect of sortilin overexpression on myogenesis is dependent on the existence of functional p75NTR that has an ability to form the high-affinity proNGF receptor with sortilin.

Physiological Significance of Endogenous Sortilin Expression in Myogenic Differentiation of C2C12 Cells—Because sortilin expression was markedly up-regulated during C2C12 differentiation (Fig. 1), we examined the physiological significance of sortilin expression in the process of myogenic differentiation using the siRNA-mediated gene silencing technique to decrease the expression of endogenous sortilin (Fig. 3*C*). Three of the sortilin sequence-specific siRNA oligonucleotides (*Oligo #1*, *#2*, and *#3*) significantly reduced endogenous sortilin expression at Day 2 of C2C12 differentiation (Fig. 3*C*, *upper panel*, *lanes 1–3*), resulting in a concomitant suppression of myogenin expression (*middle panel*, *lanes 1–3*), whereas a control scramble oligonucleotide had no effect on the expression of

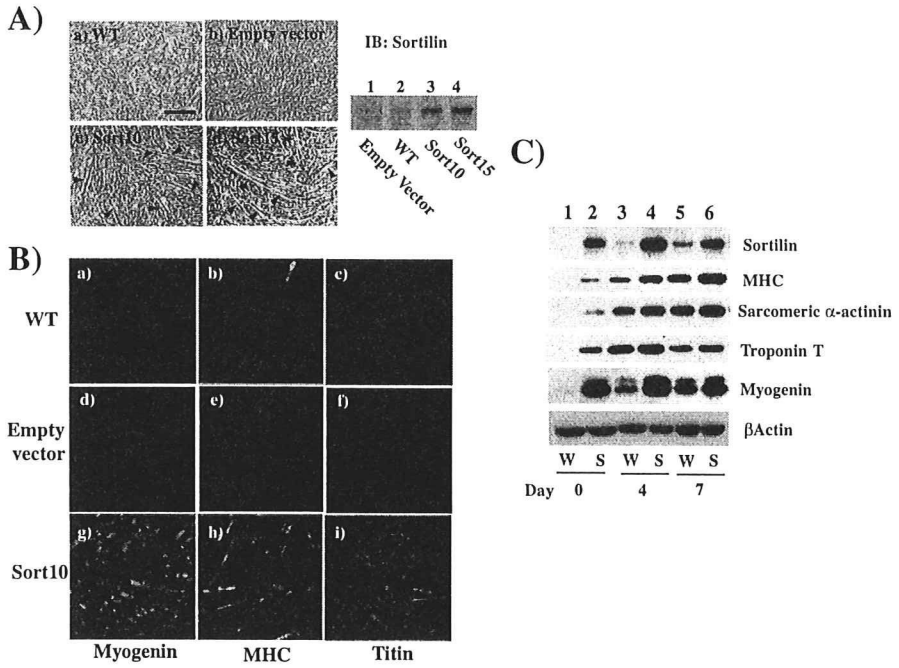

FIGURE 2. **Sortilin overexpression induces spontaneous myogenic differentiation of C2C12 cells.** *A*, parental (WT, *panel a*), empty-vector-expressing (*panel b*) and sortilin-overexpressing (Sort10, *panel c*; Sort15, *panel d*) C2C12 cells were grown to confluence (Day 0). Myotubes are indicated by *arrowheads*. *Images* are representative fields of view from three independent experiments. *Scale bar* = 300 μm. Exogenously expressed sortilin in each C2C12 cell culture was detected by Western blotting analysis (*right panel*). *B*, WT (*panels a–c*), empty vector (*panels d–f*), and Sort10 (*panels g–i*) C2C12 cells at Day 0 were fixed and subjected to immunofluorescent staining using mouse monoclonal anti-myogenin (*panels a, d,* and *g*), anti-MHC (*panels b, e,* and *h*), and anti-titin (*panels c, f,* and *i*) antibodies, which were visualized with Alexa488-conjugated secondary antibody (*green*). Nuclei were stained by 4′,6-diamidino-2-phenylindole (*blue*). *Images* are representative fields of view from three independent experiments. *C*, whole cell lysates were obtained from WT (*lanes 1, 3,* and *5*) and Sort10 (*lanes 2, 4,* and *6*) C2C12 cells on the indicated days after differentiation and total protein extracts (25 μg/lane) were subjected to Western blot analysis using antibodies against sortilin, MHC, sarcomeric α-actinin, troponin T, and myogenin. β-Actin was used as a loading control. These are representative immunoblots obtained from three independent experiments.

either sortilin or myogenin (*lane 4*). β-Actin, used as a loading control, was unaffected by siRNA introduction (*lower panel*). In addition, consistent with the sortilin overexpression experiments (Fig. 3*A*), either p75NTR- or NGF-neutralizing antibody also significantly inhibited the conventional differentiation process of wild-type C2C12 cells in a low serum differentiation medium (Fig. 3*D*). These data indicate that endogenous sortilin up-regulated during myogenesis is directly involved in the myogenic differentiation of C2C12 cells, a process possibly mediated through the proNGF-p75NTR autocrine loop.

Involvement of ROCK in the Spontaneous Differentiation of Sortilin-overexpressing C2C12 Cells—Since the p75NTR has been shown to activate the small G-protein Rho and its downstream effector ROCK in various cell types (40, 41), we examined whether this signaling cascade is involved in the spontaneous differentiation of sortilin-overexpressing C2C12 cells (Fig. 3*E*). The myogenin expression observed in sortilin-overexpressing C2C12 cells at Day 0 was diminished when the cells were cultured for 24 h in the presence of an inhibitor of ROCK, Y27632 (Fig. 3*E*, *lower panel*).

Overexpression of Sortilin Contributes to Development of an Insulin-induced Glucose Transport System in C2C12 Cells—To assess whether an insulin-responsive glucose transport system develops in skeletal muscle C2C12 cells under the same conditions as previously reported (12), WT- and Sort10-C2C12 myoblasts expressing Myc-GLUT4-ECFP were obtained using an adenoviral vector, and 2-deoxy[^{3}H]glucose (Fig. 4) and Myc Ab (Fig. 5) uptake assays (35) were then performed. Because Sort10-C2C12 cells tend to undergo spontaneous myotubular formation, we carried out the assay before they reached confluence (Day −1). Nevertheless, some differentiation markers were already being expressed at this time point (data not shown). Under the conventional 2-deoxy[^{3}H]glucose uptake assay protocol (42), insulin-induced augmentation of 2-deoxy[^{3}H]glucose uptake was not observed in either WT-C2C12 myoblasts (Fig. 4*A*, *WT*) or WT-C2C12 myoblasts expressing exogenous Myc-GLUT4-ECFP (Fig. 4*A*, *WT+G4*). Intriguingly, in Sort10-C2C12 myoblasts, basal 2-deoxy[^{3}H]glucose uptake was remarkably decreased, by ~25% (2.89 ± 0.2 pmol/min/mg of protein) as compared with that of WT-C2C12 myoblasts, whereas Sort10-C2C12 myoblasts failed to display any insulin responsiveness probably due to negligible expression of GLUT4 (Fig. 4*A*, *Sort*). However, consistent with a previous study using 3T3 fibroblasts (12), a slight but significant insulin-stimulated 2-deoxy[^{3}H]glucose uptake (~1.5-fold) was observed in Sort10-C2C12 myoblasts expressing Myc-GLUT4-ECFP (Fig. 4*A*, *Sort+G4*). This occurred concurrently with a small increase in basal 2-deoxy[^{3}H]glucose uptake.

Effects of sortilin overexpression on insulin-induced glucose uptake were also examined in differentiated C2C12 myotubes (Days 5–6) (Fig. 4*B*). Because differentiated C2C12 myotubes contain massive amounts of various muscle proteins such as skeletal muscle type myosins and α-actin, normalization by total protein contents for comparing glucose uptake between myoblasts and myotubes may not directly reflect the actual capacity for glucose transport into individual cells. However, it should be noted that the net amount of 2-deoxy[^{3}H]glucose uptake was remarkably low (1.26 ± 0.1 pmol/min/mg of protein) in differentiated C2C12 myotubes, being nearly 10-fold lower than that in undifferentiated C2C12 myoblasts (Fig. 4, *A* and *B*). Consistent with our previous report (35), insulin-induced 2-deoxy[^{3}H]glucose uptake was marginal even in differentiated C2C12 myotubes (Fig. 4*B*, *WT*) under the conventional uptake assay protocol. The adenovirus-mediated expression of Myc-GLUT4-ECFP

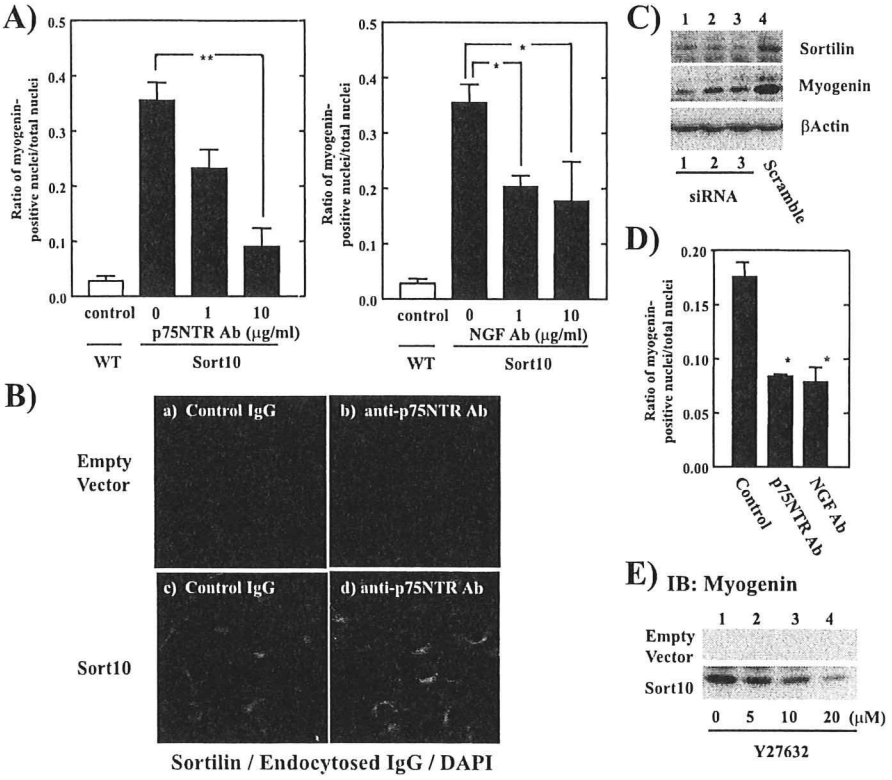

FIGURE 3. **Involvement of sortilin-p75NTR-proNGF autocrine loop in the process of C2C12 differentiation.** *A*, WT (*open bars*) and Sort10 (*solid bars*) C2C12 cells on Day −1 with the addition of either control IgG, anti-p75NTR-neutralizing antibody (*left panel*), or anti-NGF-neutralizing antibody (*right panel*), followed by culture for an additional 24 h. The cells were then fixed and subjected to immunofluorescent staining using mouse monoclonal anti-myogenin visualized with Alexa594-conjugated secondary antibody. Nuclei were stained by 4′,6-diamidino-2-phenylindole, and the number of myogenin positive nuclei was counted. The ratio of myogenin-positive nuclei out of total nuclei was expressed as the mean ± S.E. of four independent experiments. *, $p < 0.05$; **, $p < 0.01$. *B*, empty vector (*panels a* and *b*) or Sort10 (*panels c* and *d*) C2C12 cells seeded in an 8-well slide chamber were treated with 10 μg/ml of anti-p75NTR antibody or mouse IgG before they reached confluence, followed by culture for an additional 24 h. To detect incorporated IgGs, the cells were subjected to immunostaining with anti-mouse IgG (*red*) and anti-sortilin antibody (*green*), as described in A). *C*, WT-C2C12 cells (Day −1) were transfected with siRNA oligonucleotides targeting sortilin (*lanes 1–3*) or control scrambled siRNA oligonucleotide (*lane 4*) by Oligofectamine for 24 h and then cultured in differentiation medium for an additional 3 days. Total protein extracts (135 μg/lane) were subjected to Western blot analysis using anti-sortilin (*upper panel*), anti-myogenin (*middle panel*), or anti-β-actin (*lower panel*) antibodies. *D*, confluent WT-C2C12 cells were cultured in differentiation medium in the absence or presence of 10 μg/ml of either control IgG, anti-p75NTR or anti-NGF antibodies for 48 h. The ratio of myogenin-positive nuclei was assessed by immunostaining analysis as described in *A*. *E*, empty vector (*upper panel*) or Sort10 (*lower panel*) C2C12 cells were incubated with or without the indicated concentrations of Y27632 for 24 h. The whole cell lysates were then subjected to Western blotting analysis using anti-myogenin antibody.

raised 2-deoxy[^{3}H]glucose uptake under both basal and insulin-stimulated conditions, and insulin-responsiveness was slightly improved in differentiated WT-C2C12 myotubes (Fig. 4*B*, *WT+G4*). Consistent with the result obtained in undifferentiated myoblasts expressing sortilin (Fig. 4*A*, *Sort*), differentiated Sort10-C2C12 myotubes showed a further reduction in net 2-deoxy[^{3}H]glucose uptake (Fig. 4*B*, *Sort*). Because of this suppression of basal glucose uptake, a slight but significant augmentation of insulin-induced 2-dexoy[^{3}H]glucose uptake was subsequently seen even without exogenous expression of Myc-GLUT4-ECFP (Fig. 4*B*, *Sort*), presumably reflecting glucose uptake mediated through endogenous GLUT4 translocation in differentiated Sort10-C2C12 myotubes. The adenovirus-mediated expression of Myc-GLUT4-ECFP in Sort10-C2C12 myotubes further enhanced insulin-responsiveness (2.1-fold increase in response to insulin), and this was concurrent with a slight increase in basal 2-deoxy[^{3}H]glucose uptake (Fig. 4*B*, *Sort+G4*).

Effect of Sortilin Overexpression on Insulin-induced GLUT4 Translocation in C2C12 Cells—To confirm that insulin-induced 2-deoxy[^{3}H]glucose uptake was in fact achieved through the translocation of GLUT4 to the plasma membrane, the amount of Myc-GLUT4-ECFP exposed to the cell surface during insulin stimulation was assessed using an anti-Myc antibody (Myc Ab) uptake assay (Fig. 5) (35). The serum-starved WT- or Sort10-C2C12 myotubes expressing Myc-GLUT4-ECFP (Days 5–6) were incubated for 1 h in KRPH buffer containing 4 μg/ml Myc Ab in the absence (Fig. 5, *lanes 1* and *3*) or presence (*lanes 2* and *4*) of insulin (100 nM), and whole cell lysates were then subjected to SDS-PAGE followed by Western blotting using antibodies against anti-mouse IgG for detecting Myc Ab uptake and anti-BD-living colors for detecting the total amount of Myc-GLUT4-ECFP expressed. Consistent with our previous report (35), a small but significant increase in the uptake of Myc Ab was observed with insulin stimulation in WT-C2C12 myotubes expressing Myc-GLUT4-ECFP (Fig. 5, *upper panel*, *lanes 1* and *2*). Importantly, insulin-responsive GLUT4 translocation as assessed by the Myc Ab uptake assay appears to be significantly improved in Sort10-C2C12 myotubes (Fig. 5, *lane 4*), despite marked suppression of net 2-deoxy[^{3}H]glucose uptake in comparison with WT-C2C12 myotubes (Fig. 4*B*). Together, these data clearly demonstrate that sortilin overexpression improves insulin-responsive glucose transport by increasing insulin-responsive GLUT4 translocation in C2C12 myotubes. Our data also indicate the importance of decreased basal glucose uptake in the emergence of markedly increased insulin-responsive glucose uptake.

Effects of Sortilin Overexpression on Expressions of GLUT1 and GLUT4 in C2C12 Cells—Because sortilin overexpression markedly decreased basal glucose uptake (Fig. 5) and also appeared to stimulate C2C12 differentiation (Figs. 1 and 2), we examined protein and mRNA expressions of endogenous GLUT1 and GLUT4 in WT- and Sort10-C2C12 cells during

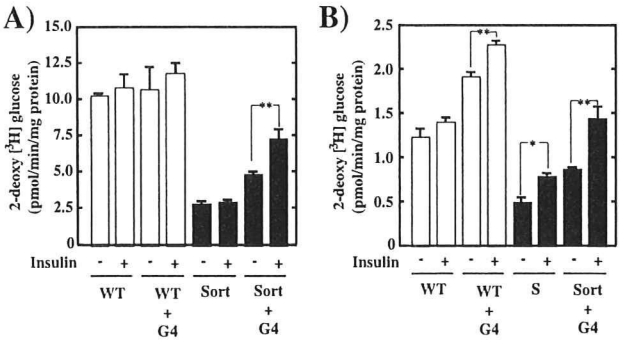

FIGURE 4. **Effects of sortilin overexpression on basal and insulin-stimulated 2-deoxy[^{3}H]glucose uptake in C2C12 cells.** *A*, undifferentiated WT (*open bars, WT*) and Sort10 (*solid bars, Sort*) C2C12 myoblasts were infected with adenovirus containing the Myc-GLUT4-ECFP gene (*G4*) or no insert. Thirty-six hours after infection, the cells were serum starved for 4 h, followed by preincubation with KRPH buffer for 10 min, and then stimulated with or without 100 nM insulin for 60 min. The cells were then subjected to the 2-deoxy[^{3}H]glucose uptake assay as described under "Experimental Procedures." Results were expressed as the mean ± S.E. of three independent experiments. *, $p < 0.05$; **, $p < 0.01$. *B*, WT (*open bars, WT*) and Sort10 (*solid bars, Sort*) C2C12 myotubes at Day 5 of differentiation were infected with adenovirus containing the Myc-GLUT4-ECFP gene (*G4*) or no insert. Thirty-six hours after infection, the cells were subjected to the 2-deoxy[^{3}H]glucose uptake assay as described in *A*. Results were expressed as the mean ± S.E. of three independent experiments. *, $p < 0.05$; **, $p < 0.01$.

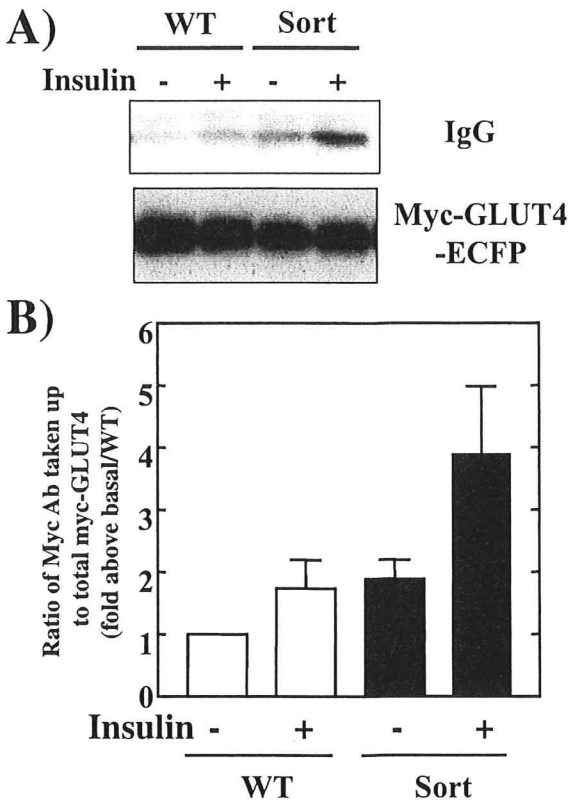

FIGURE 5. **Effect of sortilin overexpression on insulin-induced GLUT4 translocation in C2C12 cells.** *A*, differentiated WT (*open bars*) and Sort10 (*solid bars*) C2C12 myotubes at Day 5 were infected with adenovirus containing the Myc-GLUT4-ECFP gene. Thirty-six hours after infection, the cells were serum starved for 4 h, followed by stimulation with or without 100 nM insulin for 60 min. During the insulin stimulation, 4 μg of anti-Myc antibody was added to the culture. After insulin stimulation, amounts of associated/internalized antibody (*upper panel*) were analyzed by Western blotting. The total amount of Myc-GLUT4-ECFP (*lower panel*) was also analyzed by Western blotting for normalization. *B*, the results of three independent experiments were quantified using ImageJ software. Summarized results were expressed as the mean ± S.E.

myogenesis (Fig. 6). Western blot analysis demonstrated that GLUT1 protein decreased remarkably during differentiation of C2C12 cells (Fig. 6*A*, *left panel*, *lanes 1*, *3*, and *5*). Consistent with our finding that sortilin overexpression suppresses basal glucose uptake (Fig. 4), an obvious reduction of GLUT1 protein was observed in Sort10-C2C12 myoblasts (Fig. 6*A*, *left panel*, *lane 2*) as compared with that in WT-C2C12 myoblasts (*lane 1*). Upon differentiation, Sort10-C2C12 myotubes displayed marginal levels of GLUT1 protein (Fig. 6*A*, *left panel*, *lanes 6* and *7*), resulting in lower basal 2-deoxy[^{3}H]glucose uptake than that observed in WT-C2C12 myotubes (Fig. 4*B*). Real-time PCR analysis using a LightCycler (Roche Applied Science) revealed that GLUT1 mRNA expression was significantly decreased in Sort10-C2C12 cells as compared with WT-C2C12 cells even at Day 0 (Fig. 6*B*). Upon differentiation, expression of GLUT1 mRNA reached minimum levels and was present in comparable amounts in WT- and Sort10-C2C12 myotubes on Days 4 and 7 (Fig. 6*B*). We have also confirmed that sortilin overexpression resulted in increased expression of GLUT4 as assessed by both Western blotting (Fig. 6*A*, *right panel*) and real-time PCR analysis (Fig. 6*B*, *right graph*). Because decreased GLUT1 and increased GLUT4 expression are important criteria for myogenesis (43, 44), these data further confirm that sortilin functions as a potent differentiation stimulator in C2C12 cells. It is also noteworthy that, despite the similar expression levels of GLUT1 mRNA in differentiated WT- and Sort10-C2C12 myotubes (Fig. 6*B*, Days 4 and 7), cellular contents of GLUT1 protein were significantly reduced in Sort10-C2C12 (Fig. 6*A*, *lanes 4* and *6*) in comparison with WT-C2C12 (Fig. 6*A*, *lanes 3* and *5*) myotubes.

To assess whether sortilin overexpression alters the stability of GLUT proteins, we next examined time-dependent changes in cellular contents of GLUT1 and GLUT4 in the presence of cycloheximide (Fig. 6*C*). Consistent with a previous report (12), GLUT4 protein displayed greater stability in sortilin-overexpressing C2C12 myoblasts (*right panels*). On the other hand, we found that GLUT1 tended to be less stable in sortilin-overexpressing cells (*left panel*). Taken together, these data indicate that, in addition to the translational regulation, post-transcriptional regulation of GLUT1 protein is also altered by sortilin overexpression.

Increased Ubc9 Expression in Sort10-C2C12 Cells—Cellular contents of GLUT1 and GLUT4 are reportedly regulated post-transcriptionally by exogenous Ubc9 expression in the L6 skeletal muscle cell line (45). We therefore examined expression levels of Ubc9 by Western blotting (Fig. 7*A*) and real-time PCR analysis (Fig. 7*B*) in WT- and Sort10-C2C12 cells during myogenesis. We found that the amount of Ubc9 protein was significantly increased in Sort10-C2C12 cells (Fig. 7*A*, *lanes 2*, *4*, and *6*) as compared with WT-C2C12 cells (*lanes 1*, *3*, and *5*) at all differentiation time points examined. Consistent with this, a slight increase in Ubc9 mRNA expression was also observed in Sort10-C2C12 cells (Fig. 7*B*, *closed*